2023

Characterizing the Roles of Toll7 in the *Gryllus* Bimaculatus Peripheral Nervous System Development

Rowland Luo
Bowdoin College

Characterizing the Roles of Toll7 in the *Gryllus* Bimaculatus Peripheral Nervous System Development

An Honors Paper for the Program of Neuroscience

By Rowland Luo

Bowdoin College, 2023

Abstract

The study of neuronal development could provide foundational information on neurogenesis and neuroplasticity. The small size and relatively simple nervous system of Orthoptera make them ideal models for neurodevelopmental studies. The peripheral nervous system development is an intricate and precise process that each sensory neurons are able to reach their central nervous system partners in a relatively short amount of time. Although the peripheral nervous system in limb buds and their genetic regulations are well understood in grasshopper embryos, few studies have explored the developing nervous system in a cricket model. Therefore, the first goal of the current experiment is to characterize the normal peripheral nervous system development in cricket embryos. Previous studies in Drosophila have suggested Toll6 and Toll7 receptors could serve as important targets for the neurotrophic-like factors Spaetzle2 and 5. Malfunctioning neurotrophic pathways could lead to abnormal nervous system development. Therefore, the second goal of the current study is to explore the roles of Toll7 in the development of the cricket peripheral nervous system. Immunohistochemical staining using anti-horseradish peroxidase (Anti-HRP) was used to illustrate crickets' embryonic developing peripheral nervous system in the limb buds from developmental stage 7.0 to 11.0. Cricket eggs were injected with Toll7 double stranded RNA (dsRNA) and rhodamine dye to suppress the Toll7 mRNA level. The control eggs were injected with GFP dsRNA and rhodamine dye. The peripheral nervous system development in cricket embryos is largely homologous to that observed in grasshopper embryos. All later-emerged sensory neurons followed the pathway established by the first pioneer neuron Ti1. Ti1 made stereotypical turns following the steering signals on epithelial and guidepost cell surfaces and eventually fasciculate with lateral motor axons from the central nervous system. When examining the peripheral nervous system development with Toll7 knockdown, a decrease in limb bud volume was observed at stage 7.7 and stage 8.0, suggesting Toll7's potential roles in aiding cell-cell intercalation processes in Orthoptera embryos. Furthermore, a delay in Ti1 pioneer neuron development was observed with Toll7 knockdown at early developmental stages, providing evidence for Toll-Spaetzle pathway's neurotrophic-like functions. The results of the current experiment provide the first description of the peripheral nervous system development in the cricket limb buds and further evidence of Toll-Spaetzle pathway's neurotrophic properties.

Introduction

Peripheral Nervous System (PNS) Development in Insect Embryos

The study of neuronal development provides powerful insights into neuronal plasticity, neurogenesis, and neuronal circuit formation. Given the suitability for both forward (from phenotypes to unknown genes) and reverse genetics (from known genes to unknown phenotypes), as well as their extensively annotated genomes, insect models have been widely used to study the development of the nervous system. Although the structure of the orthoptera nervous system is relatively simple, extremely intricate molecular networks are required for the functional connections of a large number of developing neurons. Sensory organs in the peripheral nervous system of most orthoptera species, in particular, give rise to considerable number of afferent neurons. The femoral chordotonal organ of grasshoppers, for instance, consists of more than 600 sensory neurons (Slifer and Sekhon, 1975). These neurons are all able to precisely identify their post-synaptic targets in the central nervous system (CNS) in a segmentally homologous patterns (Meier and Reichert, 1995), and this makes the investigation of the molecular mechanisms behind insect peripheral nervous system development remarkably appealing.

The development of the peripheral nervous system (PNS) has been widely studied in grasshopper embryos given their distinct and large neurons. In grasshopper embryos, as in other insects, the peripheral nervous system (PNS) develops independently of the CNS. The first peripheral nerve route is established by a unique class of pioneer neurons, whose soma lies between ectodermal and mesodermal epithelium layers at the distal tips of limbs and antennae (Bate, 1976). During early developmental stages, the newborn pioneer neuron divides in two, and both cell bodies project axons toward CNS. Filopodia filaments start to widely protrude from the axons and occupy the entire lumen as pioneer axons elongate (Goodman and Bate, 1981). The morphology of a pioneer neuron is characterized by its unidirectional unbranched apical axon (Shankland, 1981). The localization of these pioneer neurons is homologous across orthoptera, including all closely related species: Their axons match the appendages to the corresponding CNS ganglia early in embryogenesis. The nerve formed by the pioneer axons then aids the aggregation of later-emerged sensory organ neurons and they also serve a guidance role to direct sensory axons into the CNS (Shankland, 1981). Sensory axon aggregation will be greatly disrupted if pioneer axons are ablated before nerve formation (Edwards et al., 1981).

Upon pioneer axons reaching the CNS, the sensory axons will begin to branch repeatedly until the later embryonic stages (Shankland, 1981).

In grasshopper embryos, the first pair of pioneer neurons appear at the distal tips of limb buds and antenna; the second pair of pioneer neurons appear near the base of the limb buds and antenna posterior to the first pair of pioneer neuron at around 33% development (Bentley and Keshishian, 1982). The first pair of pioneer neurons Ti1 extend axons initially along the epithelial wall, and they take two prominent turns as development progresses: the axons would first turn posteriorly toward the ventral epithelium, and then medially toward the CNS (Bentley and Keshishian, 1982). The guidepost cells and the "rules of adhesion hierarchy" are what makes pioneer neuron's unique pathfinding possible. Bentley and Keshishian (1982) found that there are three "guidepost cells" (F1, F2 and CT1) that emerge around the same time the first pair of pioneer neurons were born when no other neurons can be detected through anti-HRP staining. These cells happened to be located at the turning points of pioneer axons, indicating their cardinal roles in aiding pioneer axonal guidance. Berlot and Goodman (1984) subsequently proposed the "adhesion hierarchy" model to further explain the stereotypical pioneer axonal pathways. The protruding pioneer axons are initially guided by the adhesive signals on the epithelium. As the pioneer axons reach the guidepost cells, the adhesive signals on the guidepost cells and CNS neurons surpass that on the epithelium, thereby redirecting the pioneer axons away from epithelial walls and aiding the formation of the observed stereotypical pioneer axonal pathways.

Although the peripheral pioneer development in grasshopper embryos has been thoroughly studied, few studies have described the pioneer neuronal development in cricket limb buds. Like grasshopper embryos, the pioneer neurons in cricket appendages are large and recognizable and can be easily visualized through anti-horseradish peroxidase (anti-HRP) immunohistochemistry staining. Sufficient evidence shows that the molecular pathways regulating peripheral nervous system development emerged about 300 million years ago and have since been conserved in various orthoptera species (Meier and Reichert, 1995). Therefore, the developmental patterns observed in grasshopper models are likely parallel to the cricket models. Furthermore, Donoughe and Extavour (2016) described 24 stages of embryonic cricket development, along with a detailed timeline of when those developmental characteristics usually

appear. The Donoughe and Extavour timeline, therefore, can be used as a reliable reference to study cricket peripheral nervous system development.

Understanding the Role of Toll7 in Cricket Embryonic Nervous System Development

Some proteins work as developmental cues serving as chemical attractants or repellants to guide axonal growth cones to their desired target locations. The discovery of trophic-like functionality of the Spaetzle (Spz) and Toll signaling pathway in Drosophila raises the potential role of Toll receptors as developmental cues (Lewis et al., 2013). Toll receptors were first recognized as pattern recognition receptors (PRRs) in Drosophila as a part of the innate immune system. However, extracellular protein Spaetzle binding to the leucine-rich repeat (LRR) domains of Toll receptors can also cause their activation. Although the Toll-Spaetzle pathway was found to have certain immune properties in which it activates the transcription of anti-fungal peptides (Imler & Hoffmann, 2001), Spaetzle was also found to be structurally similar to human nerve growth factors, indicating its potential role in neuroplasticity and neurogenesis (Parthier et al., 2014). Indeed, many studies have confirmed the trophic-like properties of the Toll-Spaetzle pathway. For instance, the loss of Spaetzle 3 (Spz3) in Drosophila results in the glial ensheathment deprivation, causing increased neuronal deaths, indicating the role of the Toll-Spaetzle pathway in neuronal survival (Coutinho-Budd et. al, 2017). Furthermore, Spz mutant fruit flies show decreased bouton activity and decreased neuromuscular junction (NMJ) terminal density (Sutcliffe et al., 2013), suggesting a role for the Toll-Spaetzle in synaptogenesis.

Among the Toll receptors, Toll6 and Toll7 receptors are expressed in Drosophila embryonic nervous system. While Toll6 was found to be expressed in a small subset of neurons in the central nervous system, Toll7 is expressed in a much larger subset of neurons in both CNS and especially the leg imaginal disc (Kambris, et. al, 2002). Furthermore, Toll7 stands out due to evidence supporting its potential role in axonal guidance. Toll7 receptors are expressed throughout development in Drosophila nervous system. Spaetzle-2 and Spaetzle-5 bind to Toll6 and Toll7 promiscuously, regulating locomotion, axon targeting, and cell survival (Mclloy et al., 2013). Moreover, RNAi knockout of Toll7 in Drosophila olfactory organs results in the mistargeting of olfactory receptor neuron axons and projection neuronal dendrites (Ward et al., 2015). Our lab confirmed the existence of Toll7 in cricket embryos from stage 6 to stage 10 with both PCR and qPCR, identifying an increase in expression of both across embryonic development. In contrast to Drosophila, *in situ* hybridization experiments in crickets found Toll7

expression mainly in bands in the embryonic limb buds, suggesting a role in PNS development (Al Musawi and Horch, 2022). As of now, few studies have examined the roles of Toll7 in the developing peripheral nervous system. Thus, the goal of this study is to explore the potential roles of Toll7 in cricket peripheral embryonic nervous system development.

Experimental Design

To study the roles of Toll7 receptors in the development of the peripheral nervous system, control eggs were injected with double stranded RNA (dsRNA) against GFP, and the treatment eggs were injected with dsRNA targeting Toll7. GFP dsRNA-injected eggs were used as controls due to the possibility that the wounds caused by injection and the presence of dsRNA generally might impact embryonic development. Anti-HRP fluorescent antibodies were used to visualize the embryonic nervous system. Anti-HRP antibodies bind to Nervana proteins ubiquitously expressed on developing neuronal membranes, thus staining the entire developing nervous system (Sun and Salvaterra, 1995). The pioneer neurons' lengths and volumes at each developmental stage from stage 7.5 to stage 8.0 were measured with Imaris. The lengths and volumes of the GFP controls and Toll7 treatments were then compared and analyzed. Furthermore, limb bud volumes were measured to detect Toll7's possible impact on embryonic limb bud development. Before stage 7.5, most pioneer neurons have yet to emerge in the limb buds. By stage 8.5, most pioneer neurons had connected to the lateral motor projections from the CNS; therefore, it was challenging to focus on the morphology of pioneer neurons alone at this stage. As a result, in this experiment, we focused on stage 7.5 to stage 8.0 embryos. The confocal images of pioneer neurons for GFP controls and Toll7 dsRNA injected embryos were also examined and compared visually to detect any additional morphological differences. Finally, leg volumes, PN lengths and PN volumes were re-analyzed to detect any statistically significant differences among the three pairs of limb buds (pro-, meso-, and metathoracic limb buds) for both GFP controls and Toll7 knockdown embryos.

Methods

Animal Husbandry and Eggs Collection

Gryllus *bimaculatus* (Mediterranean crickets) were maintained on a 12:12 light: dark cycle. The temperature and humidity were controlled at 28 degrees Celsius and 60%-80%, respectively. The crickets were fed with water and cat chow ad libitum.

Adult crickets were deprived of water and damp dirt 12-16 hrs before egg collection. To collect eggs, a 35mm petri dish filled with tap water-soaked white playground sand was covered with a damp 18x18cm paper towel and placed inside the cricket bins. The eggs were collected

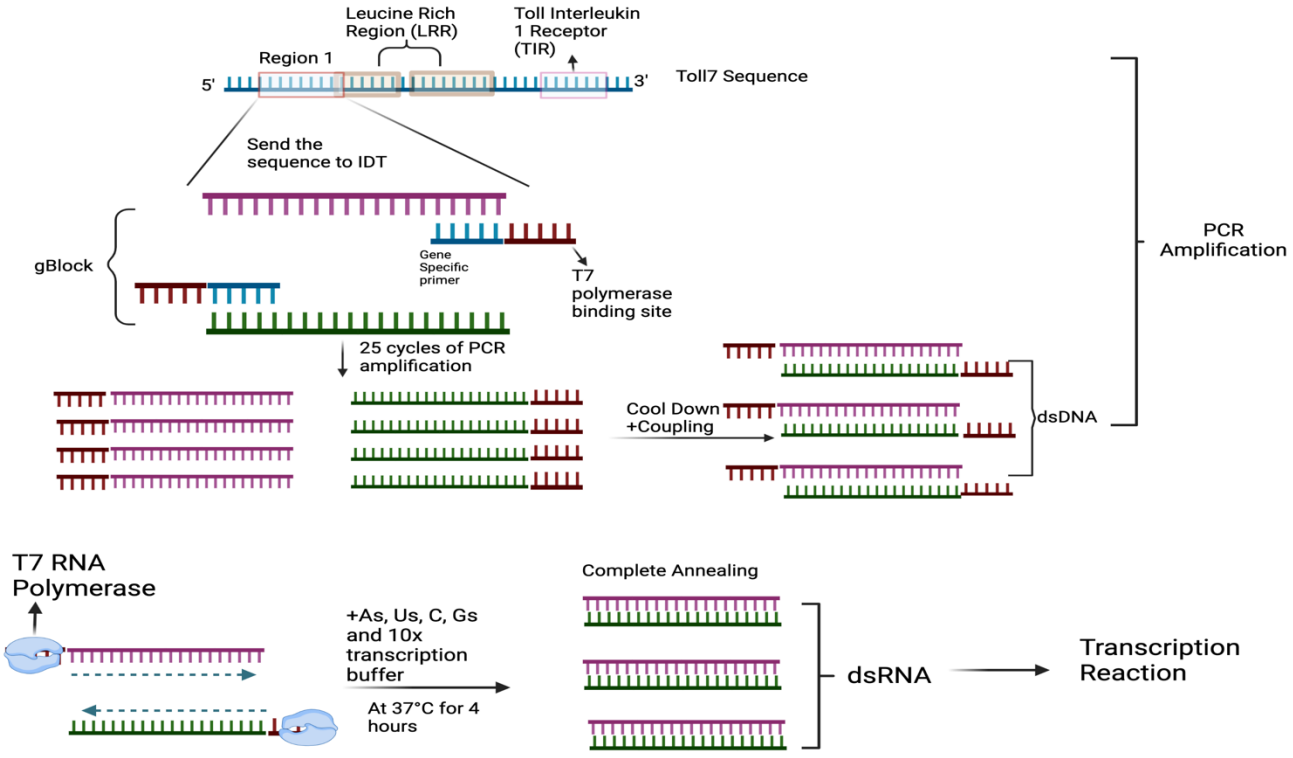

Figure 1. An Illustration of dsRNA Making Mechanisms (Created by Biorender.com). A region of sequence (region 1) that slightly overlaps the first leucine rich region (LRR) on the 5' end of Toll 7 (or GFP) sequence was selected and sent to IDT to be synthesized into a gBlock. PCR was performed in the presence of gBlock and gene specific left and right primers. Finally, transcription reaction was performed to allow the synthesis of dsRNA.

two hours later and transferred to an egg well dish made from 1% agarose in RO water. The eggs were then immersed in HBS and 1% Penicillin-Streptomycin mixture to prevent infection.

Double-Stranded RNA Synthesis

Figure 1 provides a brief description of dsRNA synthesizing process. The entire process can be subdivided into two stages: PCR and transcription. A 10x reaction was prepared for PCR. For each tube, 10uL of gBlock template, 10 uM of left and right primers each were added to 170 uM of master mix containing 283.8 uL deionized water, 44uL of 2.5 mM dNTP mix, 44uL of 10x ExTaq buffer and 2.2uL of EX-HS Taq. PCR was performed via Veriti cycler for 25 cycles, and the reaction volume was set to be 100 uL. The cycle parameters are set as following: Stage 1, 95°C for one minute; Stage 2, 95°C for 30 seconds, 56°C for 30 seconds, and 72°C for 45 seconds; Stage 3, 72°C for 4 minutes, and 4 °C for infinity. The PCR product was then confirmed on a gel electrophoresis. After confirmation, the PCR product was purified using QIAquick PCR Purification Kit. Purification procedures were performed under the QIAquick instruction sheet, and the resulting product should be in 28uL to 30uL deionized water. Next, the concentrations of PCR product were measured with Nanodrop and recorded.

For the 4x transcription reaction, in each tube, 4 ug of PCR product was added to master mix containing 8uL of each NTP (Cs, As, Gs, Us), T7 10x reaction buffer and T7 enzyme mix, as well as RNAse free water (to make the total reaction volume to be 80uL). Then, the tubes were incubated at 37°C for 4 hours on a heat block. After 4 hours, 1uL of Turbo DNAse was added to each tube to eliminate residual DNA product. All tubes were then incubated at 37°C for 30 minutes. After the last incubation, the resulting product was purified with QIAquick Purification Kit. The QIAquick instructions were followed, and the resulting eluted product should be in 14 uL RNAse free water. Finally, after confirming the product on a gel electrophoresis, the concentrations of resulting dsRNA product were measured using Nanodrop, and the concentration of dsRNA in each tube was adjusted to 3ug/uL.

Injection Needles, Beveling, and Egg Injection

The DMZ Zeitz-Puller was set to program P10 (for patch clamp pipette, thin-walled glass) and P(A) when the glass microcapillaries were pulled. The pulled microcapillaries were mounted on a Narishige beveler (Model EG-45) to be beveled for 2 to 3 minutes at a 20 degrees angle. The pulled needles were then transferred under a Leica microscope with a camera, and the diameters of the inner walls adjacent to the opening of the needles were measured with LAS

Core light visualizing software (**Fig. 2**). The needles with diameters larger than 12um or smaller than 8um were discarded. The beveled needles were then stored on a wax strip in a petri dish.

The Narishige microinjector was set to 0.17 seconds, the pressure was set to 10-15 psi, and the balance was set to zero. A mixture of 0.5 uL of rhodamine dye, 0.5 uL of injection buffer and 4 micrometers of dsRNA materials (GFP dsRNA as control, and Toll7 dsRNA as treatment) was needed for the injection of a plate of eggs (approximately 120 eggs). 1.5 mL of injection solution was loaded into the needle for each injection. The balance was for each needle was set by so that a thin stream of injection solution could be observed under the fluorescent dissecting microscope (Leica). The eggs were injected at 20% to 30% of length at the posterior end (the blunter end), which is the location of embryogenesis (Miyamoto & Shimozawa, 1983). The "clear" button was occasionally used if the needles became clogged. The number of eggs injected each day was recorded.

The plate with injected eggs was covered and stored in a warm incubator at 28 Celsius, at 60% to 80% RH. The 1% HBS-Pen/Strep suspension solution was changed daily, and deceased eggs were picked out daily to decrease infection and maximize survival rates. After two days, the injected eggs were transferred to a dish filled with five layers of paper towels soaked in HBS-Pen/Strep solution. The dishes were stored in the cricket incubators, with paper towels changed and dead eggs removed daily. The survival rates of the injected eggs were monitored daily, with the day the eggs were laid being recorded as Day 0.

Figure 2. An Illustration of a Beveled Needle under Microscope (Created by Biorender.com). A successfully beveled needle should present an ideal oval-shaped opening. With inner walls of the microcapillary being visualized, the diameters of the needle openings should be no larger than 12 um and no smaller than 8 um.

Embryo Dissection and Fixation

Dissection of injected eggs started on Day 4 and Day 5 due to delayed development of injected embryos. Cricket embryos were found to have slightly variable developmental rates, even when laid within one hour of each other and raised under identical laboratory conditions (Donoughe & Extavour, 2016). Thus, various embryos from all stages, from stage 6.5 to stage 11, were expected to be obtained within a 5-day dissection window. The dissection was performed in PBS solution. The dissected embryos were transferred to a round bottom 2mL tube containing about 300uL 4% PFA in PBS for 25 minutes. Next, the embryos were washed with PBSTx (1X PBS containing 0.1% TritonX-100) for 3x5 minutes. Then, the embryos were transferred to 1mL PBSTx containing a round-bottom tube and stored at 4°C cold room.

Embryonic Stage Determination

The embryonic stages were determined upon dissection based on Donoughe and Extavour (2016)'s descriptions of eggs' external appearances under brightfield microscope as

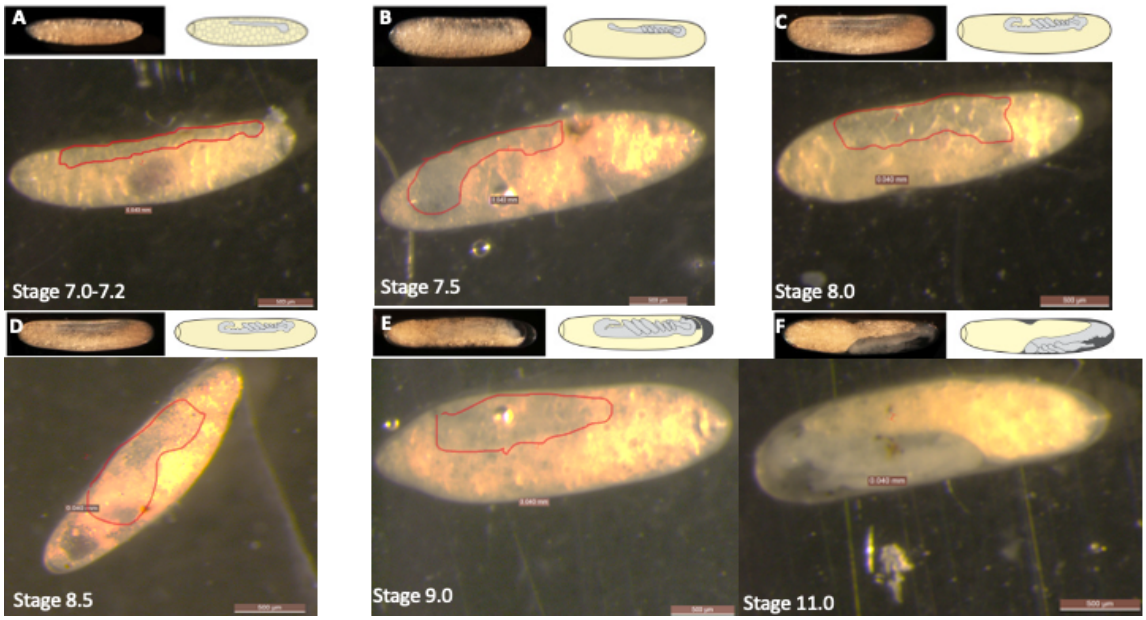

Figure 3. Examples of Eggs from Various Stages. For each panel, the smaller pictures are obtained from Donoughe & Extavour (2016), and the bigger pictures are egg examples used in the current experiment. The eggs' shape and tautness, as well as embryonic sizes and intra-zygote locations were examined and compared with the exemplar provided by Donoughe & Extavour. The red trace roughly outlines the embryos in the eggs. It is notable that the embryonic shape, size and positions go through stereotypical changes throughout development.

well as the length of embryonic antennas and the shape of limb buds. Pictures of the eggs were acquired prior to dissection with Leica LAS Core software and compared with Donoughe and

Extavour (2016)'s egg pictures and schematic drawings at different developmental stages (**Fig. 3)**.

Immunohistochemistry, Slide Mounting, and Visualization

The stock concentration of Alexa Fluoro594-conjugated anti-mouse HRP was 1.5 mg/ml in DMSO. The antibodies were diluted separately with PBSTx-HS (10% horse serum in PBSTx) solution so that the final concentration of the antibodies was 1:400. After rinsing the fixed embryos with PBSTx solution for 3x5 minutes, they were immersed in PBSTx-HS solution for blocking for one hour. The embryos were then incubated with anti-HRP primary antibodies overnight on a shaker in the cold room (4 Celsius degree). Embryos were rinsed with PBSTx for 3x5 minutes and then mounted with 50% glycerol in PBS.

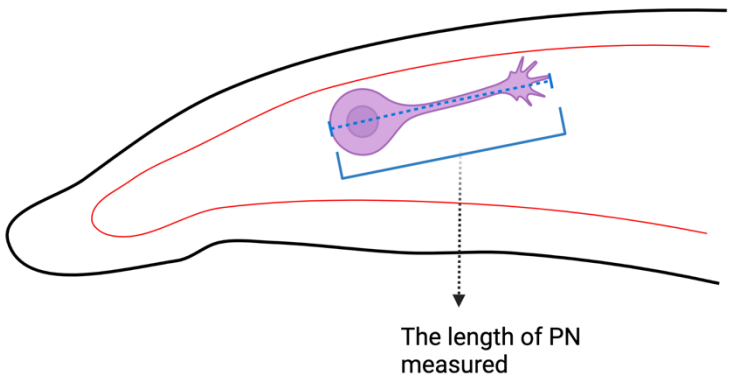

Figure 4. A Schematic Drawing of a Cricket Embryonic Limb Buds with Pioneer Neuron and the Measurements Used in This Experiment (Created by Biorender.com). The length of the pioneer neuron (PN) was measured from the furthest point on the cell bodies to the furthest point of the growth cone.

Embryos were visualized with Leica DM6 CS confocal microscope and subsequently visualized with LAS Core software. Images (40x) focusing on the prothoracic, mesothoracic and metathoracic limb buds were acquired for each embryo.

Data Analysis

All confocal images were analyzed blind-to-condition with Imaris software. The pro-, meso-, and metathoracic pioneer neurons' lengths and total volumes were measured for each embryo staged 7.5 to 8.0 (**Fig. 4**). When measuring the lengths of pioneer neurons, 10 to 20

reference points about equal distances were selected on the cell bodies, axons and filopodia. Then the sum of the straight-line distances for each pair of Ti1 pioneer neurons was recorded as the length of the pioneer neuron. When measuring the PN volumes, a selected region that contained the entire pioneer neuron was masked. Imaris is then able to automatically detect and select the entire pioneer neuron with background subtraction. After setting the "Smooth" value to 0.9 and manually adjust the selected region to only include pioneer neurons, the volume of the selected region would be reported. Three pairs of limb buds' volumes were also measured for each embryo from stage 7.5 to 8.0. Similar processes applied when measuring the limb bud volume. However, "absolute intensity" measurement was used instead of "background subtraction." Furthermore, due to the hollow structure of embryonic limb buds, the "Smooth" value was set to 10.0 (larger value indicates that Imaris would consider two closely positioned pixels as one signal, therefore generating a more smoothened selected structure), so that both the lumen and the epithelial volumes would be considered. Furthermore, limb buds that have long and voluminous filopodia were identified (**Fig. 5),** and the percentages of limb buds that possess this characteristic were calculated and compared between GFP controls and Toll7 knockdown groups. Pioneer neurons that were categorized as "long and voluminous" have filopodia covered the entire cell, including the cell bodies, axons, and growth cones. Moreover, the growth cone of these neurons' filopodia filaments and long and dense enough to cover the entire limb bud lumen, and they typically present branching filopodia phenotype.

Finally, all data was analyzed with Microsoft Excel and GraphPad Prism 9. Two-way ANOVA tests were performed on limb bud volumes, PN lengths and PN volumes against embryonic stages, and a post-hoc analysis was subsequently conducted. A statistical significance was determined at $p<0.05$, and a statistical trend was determined at $p<=0.20$.

Results

To study peripheral nervous system development under Toll7 knockdown conditions, normal peripheral nervous system development in the limb buds was characterized using GFP control embryos. Then, the developmental patterns were observed in Toll7 knockdown embryos, and compared with that in GFP controls.

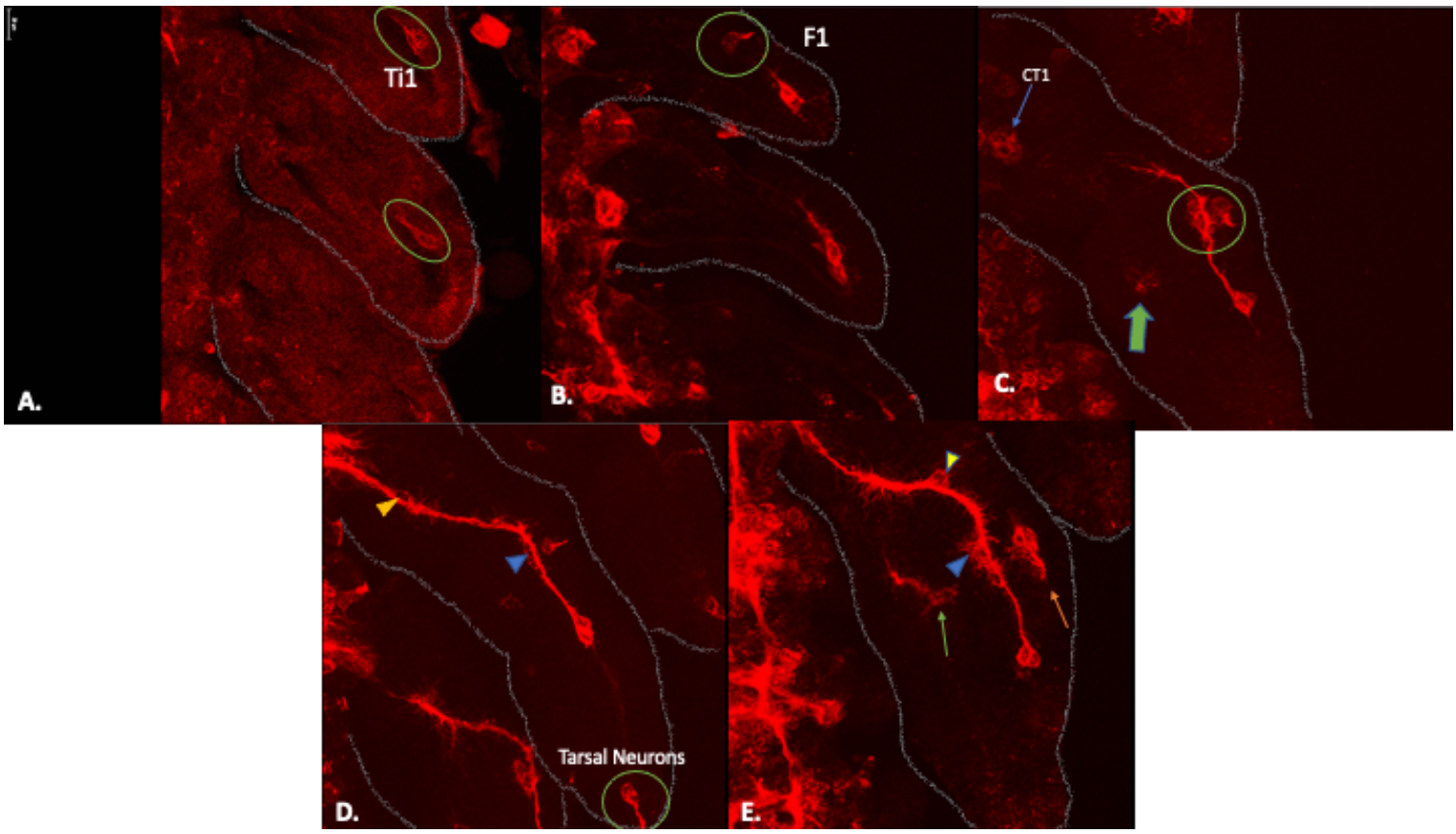

Figure 6. Normal Development of Limb Bud Nervous System from Stage 7.0 to 8.5. A. Newborn pioneer neuron pairs (Ti1, green circles) first develop under the epithelium layer from stage 7.0 to 7.2. **B.** Axons extend from spindle shaped Ti1 cell bodies along the epithelium layer toward the first guidepost cell F1 at around stage 7.5. **C.** At stage 7.7 to 8.0, Ti1 growth cone had contacted cell F1 (green circle) and made a ventromedial turn toward the second guidepost cell CT1 (blue arrow). The second pair of pioneer neurons Ti2 (green arrow) had emerged at this stage. **D.** At stage 8.5, most Ti1 axons have reached CNS. Notably, Ti1 axons make their stereotypical turns at each guidepost cells. At this stage, tarsal neurons start to emerge at the distal tips of limb buds (Yellow arrowhead: CT1 guidepost cell. Blue arrowhead: F1 guidepost cell). **E.** As Ti1 axon approached the CNS, sensory neurons (orange arrow) started to gather near F1 to form early chordotonal organs. Ti2 cells (green arrow) start to project axons dorsal-anteriorly to approach the Ti1 axon. Rapid increase in filopodia can be observed along Ti1 axons (Yellow arrowhead: CT1 guidepost cell. Blue arrowhead: F1 guidepost cell). The limb buds are outlined in grey.

The Development of the Cricket Peripheral Nervous System in the Limb Buds

The first pair of pioneer neurons (Ti1) emerged beneath the dorsal epithelium layer near the distal end of the limb buds at around stage 7.0 to 7.2. Within a two to three hours window, the sphere-shaped pioneer cell bodies started to taper at one end, forming into a distinctive spindle shape (**Fig. 6A)**. This indicates the initiation of axon extension. At this stage, Ti1 neurons were the only neurons detectable by anti-HRP labeling.

At stage 7.5 to stage 7.7, pioneer axons visibly elongated along the dorsal epithelium layer, and the first guidepost cell could be detected with anti-HRP labeling around 30 μm medial to the Ti1 growth cone on the same three-dimensional plane (**Fig. 6B).** At stage 7.7 to stage 8.0, Ti1 axons had reached the first guidepost cell F1, and a sharp ventral turn was taken as Ti1 axon exits F1. At this stage, the second guidepost cell (CT1) had emerged at the base of the limb buds ventromedial to Ti1 and F1 cell bodies, and the Ti1 growth cone could be observed to evidently turn toward the newly born CT1 cell. At the same time, the cell bodies of the second pair of pioneer neurons (Ti2) could be detected with anti-HRP labeling ventroposterior to Ti1 neurons (**Fig. 6C).** Between stage 8.0 and 8.5, lateral motor neurons (LMNs) from the CNS started to extend growth cones toward guidepost cell CT1 while Ti1 axons progressively approached CT1 cell bodies. Eventually, Ti1 growth cone reached CT1 and subsequently followed the axonal path established by the "CT1-LMN" connection to the CNS. By the time Ti1 axons make their initial contact with the CNS cells, tarsal neurons (Ta) at the tip of each limb bud started to emerge and rapidly divided into spindle-shaped cells (**Fig. 6D).** Soon after the completion of Ti1 contact to the CNS, a rapid growth in neuronal number was detected. The second pair of pioneer neurons (Ti2) started to extend axons toward Ti1 axons. Femoral chordotonal organ (FCO) neurons started to gather at F1 cell. A prominent increase in axonal filopodia could be observed on both Ti1 and Ti2 axons (**Fig. 6E).**

From stage 8.5 to stage 9.0, sensory organs visibly enlarged. It could be observed that femoral chordotonal organ (FCOs) neurons, which were co-localized with F1 guidepost cells began to form their typical rod-like shapes and were arranged vertically to form a fan-like shape. Sensory organ complex (SOK) started to gather at the Ti1 cell bodies. Ti2 pioneer axons were evidently elongated, with their growth cone filopodia reaching the Ti1-LMN axonal intersection, forming the first observable peripheral nerve "branch" in the limb buds. Concurrently, tarsal neurons underwent several rounds of division and initiate an axon toward the Ti1 cell bodies

along the epithelium (**Fig. 7A)**. From stage 9.0 to katatrepsis (stage 10.0), lateral motor neurons (LMNs) in the CNS rapidly underwent stereotypical axonal elongation and branching to innervate limb bud muscles **(Fig. 7B).** At stage 11.0, most sensory organs gathering had finished, and all sensory organs (femoral chordotonal organs and subgenual organs on all three pair of limbs, tracheal organs on the meso- and metathoracic limbs, and tympanal organs on the prothoracic limbs) had reached their pre-mature form. It could be observed that at this stage, FCOs on all three pairs of limb buds were separated into proximal and distal counterparts. The proximal part was characterized by a circular fan shape, while the distal part was characterized by a row of horizontally aligned rod-like sensory neurons. Tarsal neurons had formed a spiking pattern, and the tarsal axons had fully connected to the rest of limb bud peripheral nerves (**Fig. 7C).**

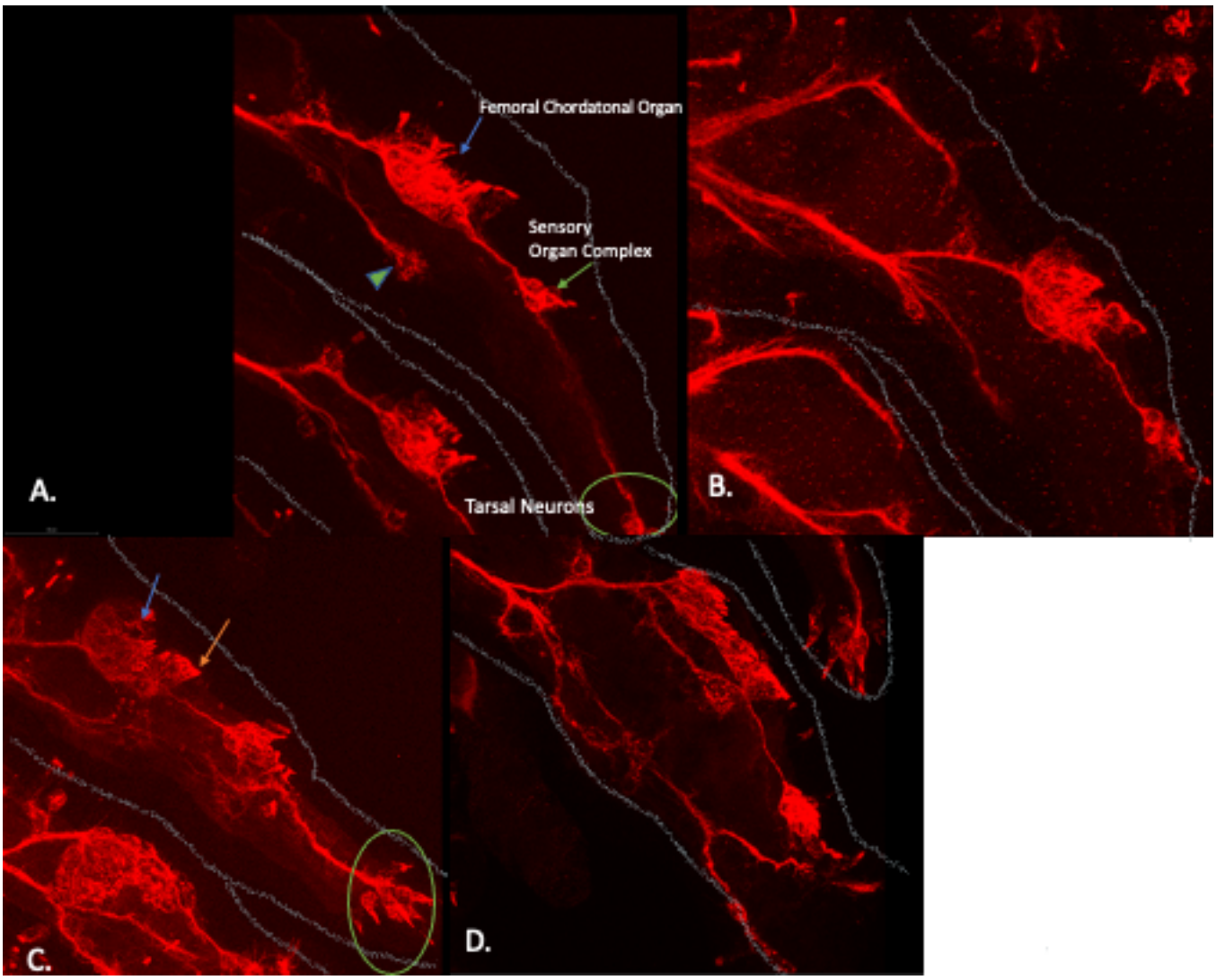

Figure 7. Development of Limb Bud Nervous System from Stage 8.5 to Stage 11.0. A. Prothoracic limb bud at stage 9.0. The femoral chordotonal organ (FCO) formed at the previous F1 guidepost cell, and sensory organ complex (SOK) neurons started to gather at the Ti1 cell bodies. Ti2 neurons' growth cone approached Ti1-LMN intersection. Tarsal neurons projected axons toward Ti1 cell bodies (green arrowhead: Ti2 cell bodies). **B.** Confocal image showing the lateral motor axons' innervation of the limb buds and their typical branching patterns at stage 10.0. **C.** Confocal image of the prothoracic limb bud at stage 11.0. At this stage, all immature sensory organs had formed, and the femoral chordotonal organ was divided into proximal and distal counterparts (blue arrow: proximal FCO. Orange arrow: distal FCO. Green circle: tarsal neurons). **D.** Confocal image showing the metathoracic limb bud at stage 11.0. Note that the distal FCO is elongated compared to pro- and mesothoracic FCOs.

The peripheral nervous system development was largely homologous in all three pair of limb buds with slight differences in the metathoracic leg. The metathoracic Ti1 cell bodies were located more distal than Ti1 cell bodies in the pro- and mesothoracic limb buds. Furthermore, the femoral chordotonal organ on the metathoracic limb bud had an elongated distal segment along the epithelial layer (**Fig. 7D).**

The Role of Toll7 in Limb Bud and Pioneer Neuronal Development in Cricket Embryos

To assess Toll7 knockdown's effects on cricket embryonic limb bud development, the volumes of each limb buds were measured and compared with GFP controls. When comparing the volumes of limb buds at all stages, a Welch two-sampled t-test showed that Toll7 dsRNA injected embryos presented a significant decrease in limb bud volumes (t=3.076, p=0.0040). First, A one-way ANOVA was performed to analyze the effect of limb bud ID (pro-, meso-, and metathoracic limb bud) on limb bud volumes at each stage. The results indicated that there were no statistically significant effects of limb bud ID on limb bud volumes (data not shown), suggesting that from stage 7.5 to stage 8.0, the sizes of the three limb buds on each embryo were roughly the same. As a result, the pro-, meso-, and metathoracic limb bud volume data were combined for further testing. A two-way ANOVA was then conduced to compare the effects of stages (stage 7.5, 7.7 and 8.0) and the dsRNA treatment (GFP dsRNA or Toll7 dsRNA injection) on limb bud volumes. The results detected a statistically significant interaction between the effects of age group and treatment conditions (F(2,59)=4.979, p=0.010). Simple main effects analysis showed that both embryonic stages (p<0.0001) and treatment conditions (p<0.0001) had a pronounced effects on limb bud volumes. Sidak's Test for multiple comparisons revealed that the mean value of limb bud volumes was statistically different between GFP and Toll7 treatment groups at stage 7.7 (p<0.0001, 95% C.I. =[5.040, 16.84]) and stage 8.0 (p=0.0157, 95% C.I.

=[0.9840, 11.95]). However, Sidak's Test for multiple comparisons failed to reveal any statistically significant differences between GFP and Toll7 treatment groups at stage 7.5 for limb bud volumes (p=0.6722) (**Fig. 8).**

To understand if Toll7 knockdown impacted PNS development, the lengths and volumes of the Ti1 pioneer neurons (Ti1 PN) were compared between GFP control and Toll7 knockdown embryos from stage 7.5 to stage 8.0. One-way ANOVAs were performed first to analyze the

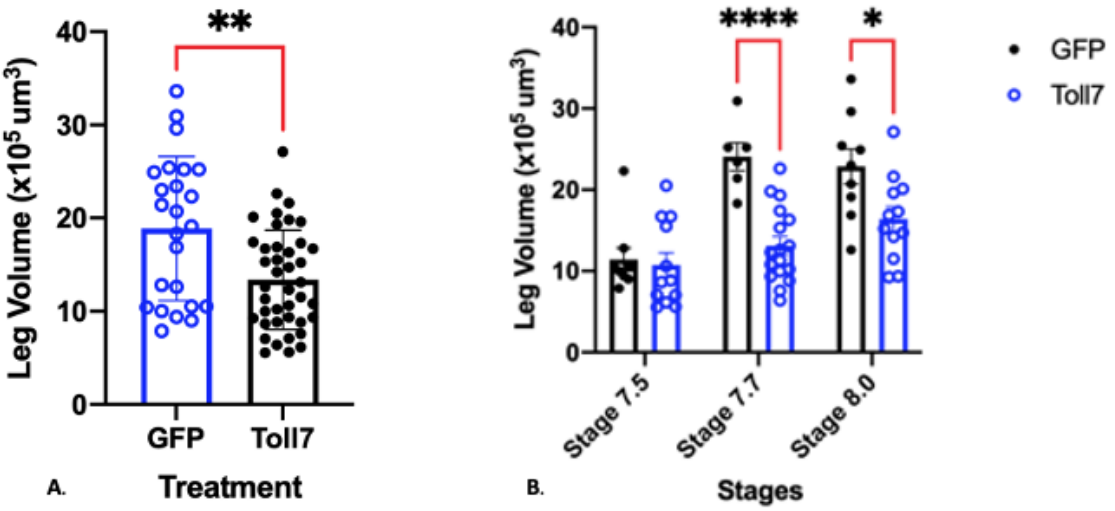

Figure 8. Toll7 Knockdown Embryos Displayed Limb Bud Volume Shrinkage. A. Toll7 knockdown embryos exhibited a significantly smaller limb bud volumes when embryos at all stages are compared together (p=0.0040). **B.** At stage 7.5, Sidak's Test for multiple comparisons showed no significant difference between GFP control and Toll7 knockdown limb bud volumes. At stage 7.7, GFP control embryos have a significantly higher mean limb bud volume than Toll7 knockdown embryos (p<0.0001). At stage 8.0, again, a statistically significant decrease in limb bud volumes was detected for Toll7 knockdown embryos (p=0.0157). All error bars in the above graphs represent standard error mean (SEMs).

effects of limb bud IDs on Ti1 PN lengths and volumes at each stage. The results of analysis failed to reveal statistically significant differences for Ti1 PN lengths and volumes among pro-, meso-, and metathoracic limb buds (data not shown). This suggested that the Ti1 pioneer neurons in each limb bud for each embryo developed at approximately the same rate from stage 7.5 to stage 8.0. Therefore, the Ti1 PN lengths and volumes for the three pair of limb buds were combined to be analyzed together. A two-way ANOVA was performed to analyze the effect of

embryonic stages and treatment conditions on Ti1 PN length and volume. The analysis revealed that there was not a significant interaction between the effects of embryonic stages and dsRNA treatment conditions for Ti1 PN length ($F(2,59)=0.1610$, $p=0.8517$). It was shown that there was a significant difference in Ti1 PN length between at least two embryonic stages ($p<0.0001$). And there was also a significant difference in PN length between the GFP and Toll7 dsRNA treatment conditions ($p=0.0056$). A Sidak's Test for multiple comparisons showed that there were no

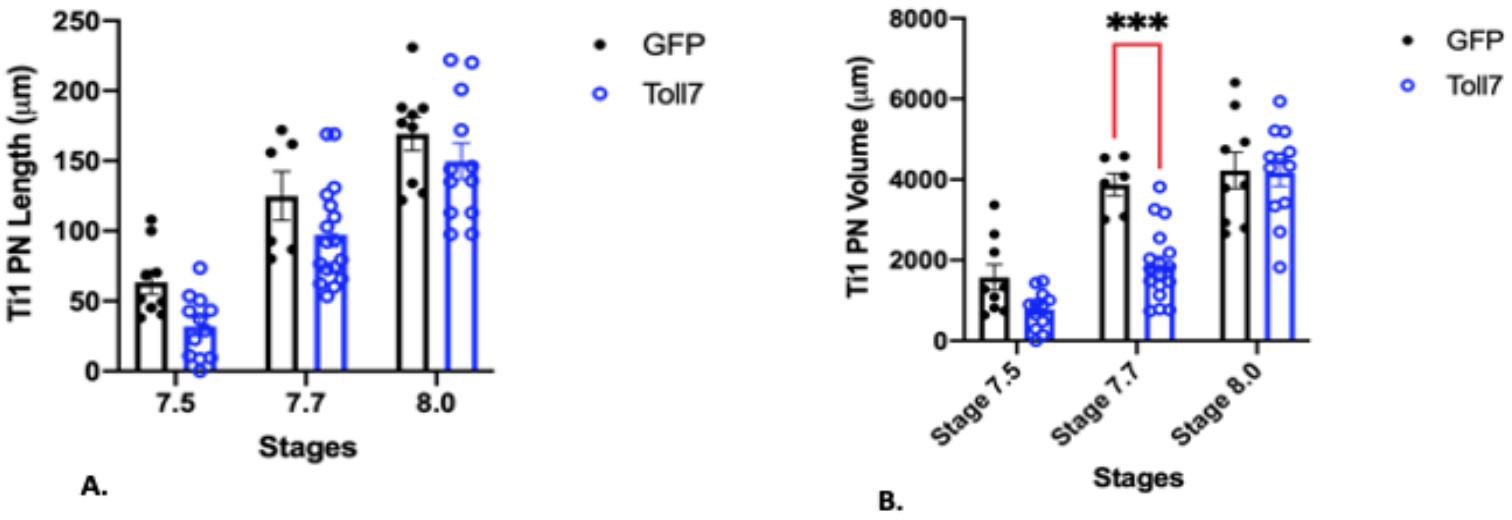

Figure 9. Pioneer Neuron (PN) Lengths and Volumes for GFP Control and Toll7 Knockdown Embryos from Stage 7.5 to Stage 8.0. A. The PN lengths tended to be smaller for Toll7 knockdown embryos compared to GFP controls ($p=0.12$) only for stage 7.5 embryos. **B.** The PN volumes are significantly smaller for Toll7 knockdown embryos at stage 7.7 ($p=0.0002$) but not at stage 8.0 and stage 7.5. At stage 7.5, Toll7 knockdown embryos tended to display a smaller mean Ti1 PN volume (p=0.18). All error bars in the above graphs represent standard error means (SEMs).

significant differences for Ti1 PN length between GFP controls and Toll7 knockdown groups at each developmental stage. However, a trend was detected at stage 7.5 that Toll7 knockdown embryos had smaller mean lengths of Ti1 pioneer neurons ($p=0.12$) (**Fig. 9A)**. A two-way ANOVA was again performed to analyze the effect of embryonic stages and treatment conditions on Ti1 PN volumes. The analysis revealed that there was a significant interaction between the effects of embryonic stages and dsRNA conditions for Ti1 PN volume ($F(2, 59)=4.893$, $p=0.0108$). Simple main effects analysis showed that embryonic stages had a

pronounced statistically significant effect on Ti1 PN volume ($p<0.0001$). Treatment conditions also had a pronounced statistically significant effect on Ti1 PN volume ($p=0.0004$). A Sidak's test for multiple comparisons illustrated that there was a pronounced significant difference between the mean Ti1 PN volume between GFP and Toll7 dsRNA treatment groups at stage 7.7 ($p=0.0002$, 95% C.I.= [867.2, 3107]), but not at stage 7.5 and stage 7.7. At stage 7.5, however, a

trending difference was detected between the mean Ti1 PN volumes between GFP controls and Toll7 knockdown groups (p=0.18) (**Fig. 9B).**

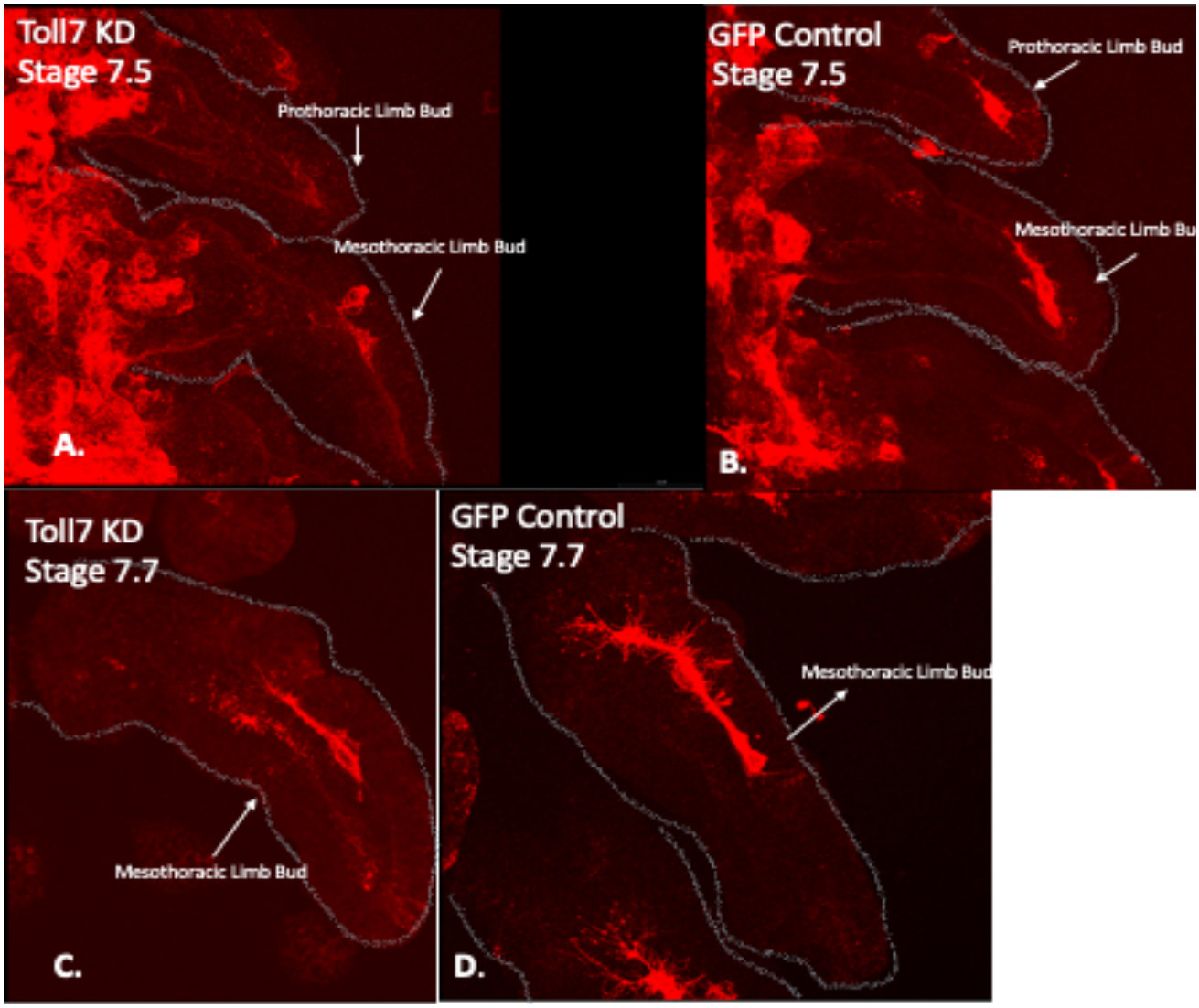

Figure 10. Confocal Images of Ti1 Pioneer Neurons at Stage 7.5 and Stage 7.7 for Toll7 Knockdown embryos and GFP Controls. A and B. Confocal images (40x) focusing on the prothoracic and mesothoracic limb buds showed a delayed Ti1 cells emergence and axonal protrusion under Toll7 knockdown. **C and D.** Confocal images (40x) focusing on the mesothoracic limb buds showed a prominent decrease in filopodia both along the axon and at the growth cone. Furthermore, unlike GFP controls, Toll7 knockdown PN has not yet reached the first guidepost cell F1 and undertaken the stereotypical ventromedial turn.

The morphology of the Ti1 pioneer neurons was also compared between the GFP controls and Toll7 knockdown embryos visually. As portrayed by the data, at stage 7.5, only newborn spherical pioneer cell bodies could be observed in Toll7 knockdown embryos, with little to no axonal protrusions. Whereas in GFP controls, most Ti1 cell bodies had extended their axons along the epithelial layer for about 50 um (**Fig. 10A-B).** At stage 7.7, most GFP control PNs had reached the first guidepost cell F1 and underwent the stereotypical ventromedial turn, while most Toll7 PNs have yet to reach F1(**Fig. 10C-D).** There was no detectable evidence of filopodia

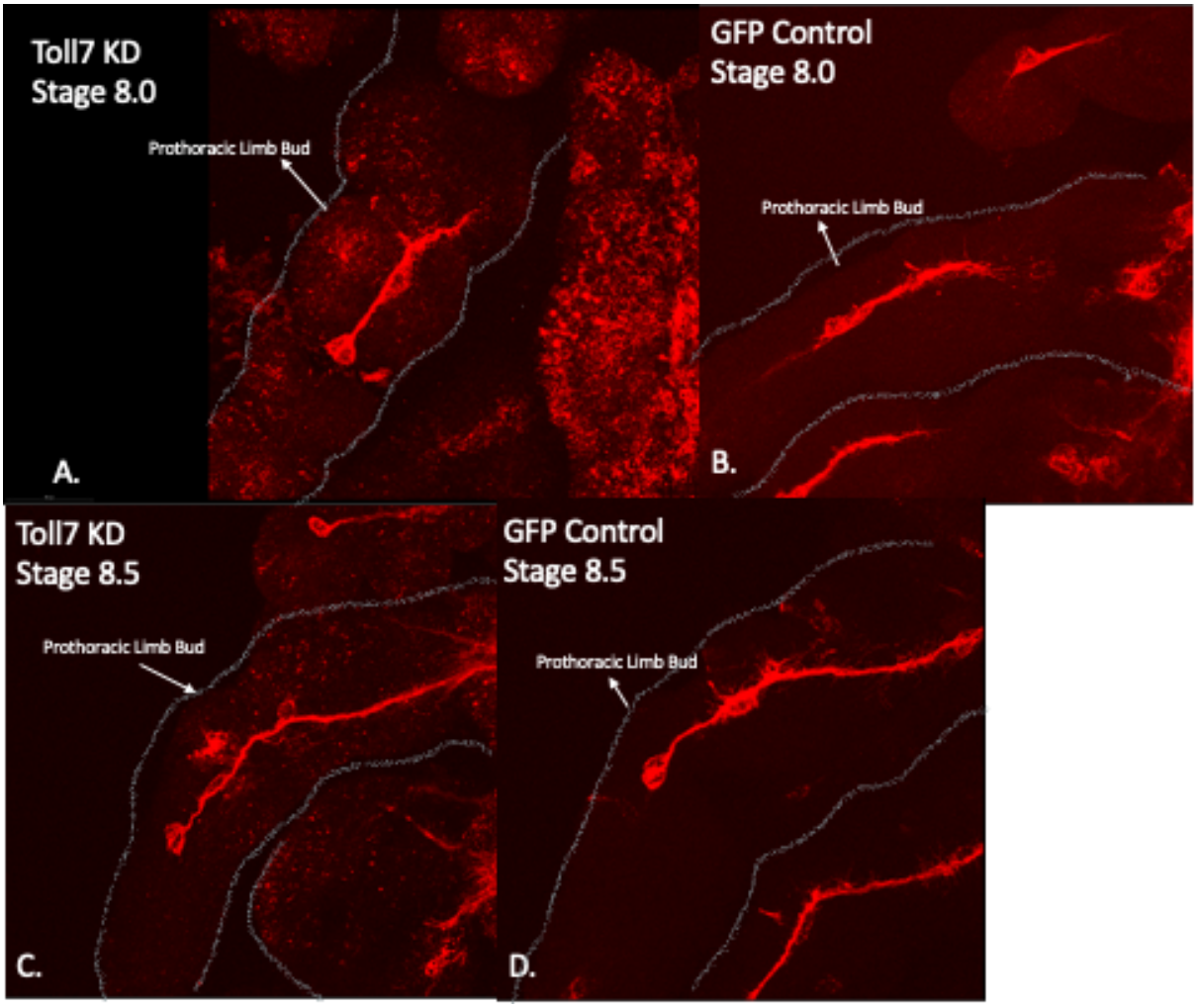

Figure 11. Confocal Images of Ti1 Pioneer Neurons at Stage 8.0 and Stage 8.5 for Toll7 Knockdown Embryos and GFP Controls. No prominent morphological differences were detected between Toll7 knockdown and GFP control embryos.

extension and exploration in Ti1 neurons in Toll7 knockdown conditions prior to stage 8.0, as compared to robust filopodia presence in the controls. Starting from stage 8.0, few

morphological differences in the pioneer neurons could be observed between GFP control and Toll7 knockdown embryos (**Fig. 11A-D).** Embryos at later stages (stage 9.0 to stage 11.0) exhibited relatively normal sensory organ gathering and sensory/motor nerve branching patterns for both GFP controls and Toll7 knockdown embryos, and the morphologies at these stages were indistinguishable (pictures not shown).

Finally, to assess whether the bigger volumes in PNs for GFP controls at stage 7.5 and stage 7.7 were due to increased filopodia number and length, the percentages of the limb buds that have PN filopodia occupying the entire lumen were calculated from stage 7.5 to stage 8.0 for both GFP controls and Toll7 knockdown embryos. At stage 7.5, 33% of GFP PNs were observed to possess filopodia that covers the entire limb bud lumen, whereas only 8% of Toll7 PNs were observed to have similar voluminous filopodia fibers. Similarly, at stage 7.7, 100% (all) of the GFP PNs possessed long, branching filopodia throughout the neurons that covers the entire lumen, whereas only 12% of Toll7 PNs exhibited similar features. At stage 8.0, however, the percentages of PNs that possess voluminous filopodia were similar between GFP controls and Toll7 knockdown embryos, with 78% of GFP controls and 68% of Toll7 knockdown embryos (**Fig. 12).** Figure 13 provides a comparison of Ti1 filopodia outgrowth at each stage for GFP controls and under Toll7 knockdown. Each panel presents a relative representative example of their respective group (**Fig. 13).**

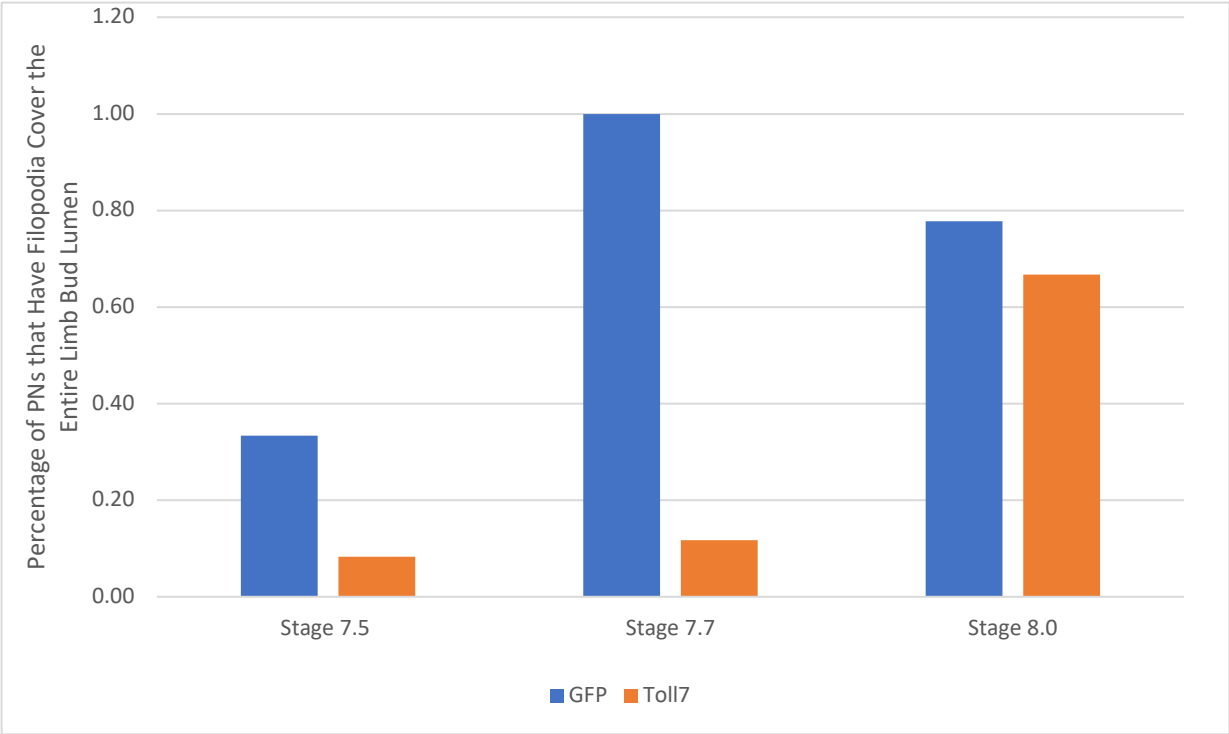

Figure 12. Percentages of PNs that Possessed Filopodia that Covered Entire Limb Bud Lumen from Stage 7.5 to Stage 8.0 for GFP Control and Toll7 Knockdown Embryos. At all three stages, Toll7 knockdown embryos presented lower percentages of PNs that possessed voluminous filopodia. However, the smaller percentages are the most prominent at stage 7.5 and stage 7.7.

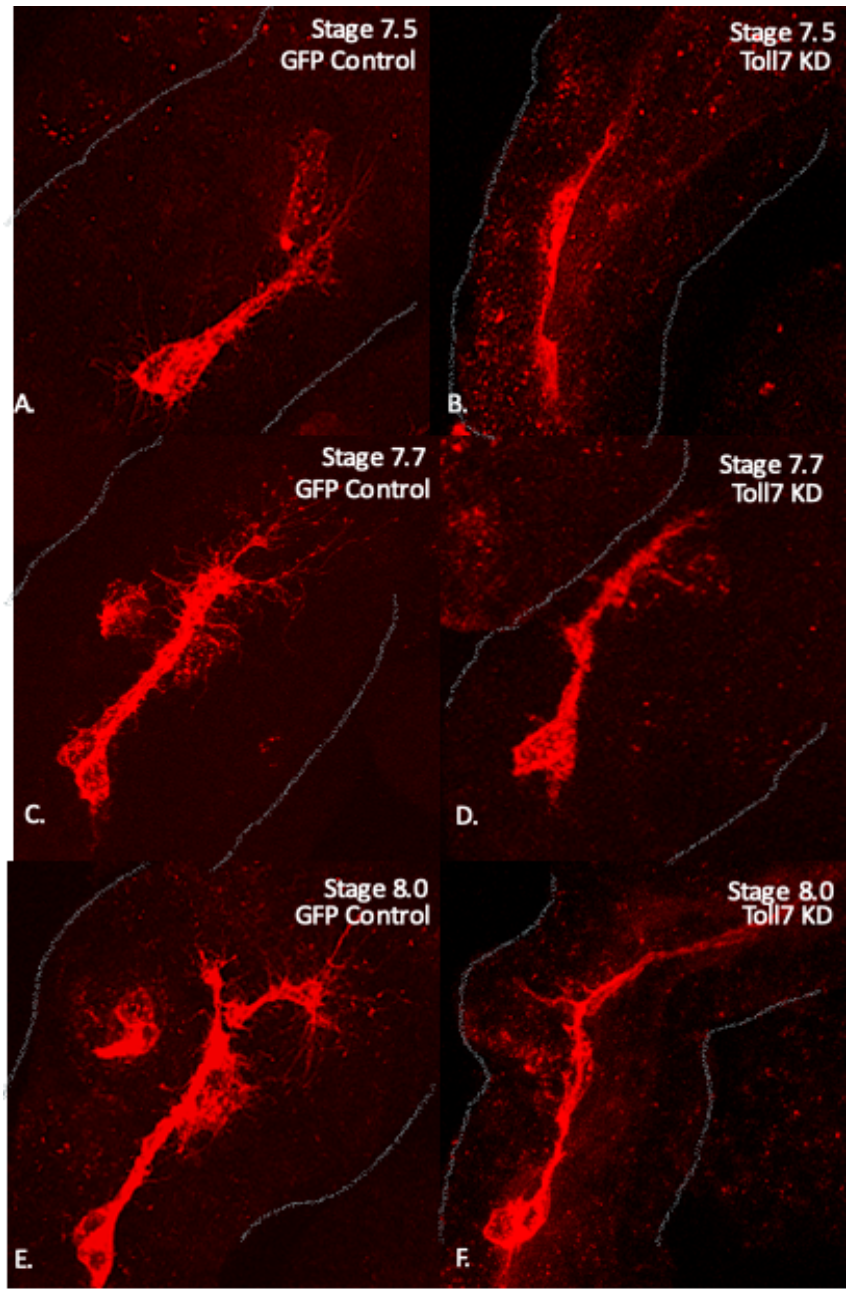

Figure 13. Toll7 Knockdown Embryos Presented Less Filopodia Outgrowth. A and B. 40x confocal images focusing on the prothoracic limb bud at stage 7.5. Filopodia can be observed throughout the pioneer cell bodies and axons for GFP control but little to no filopodia can be observed throughout the neuron for the Toll7 knockout pioneer neuron. **C and D.** 40x confocal images focusing on the prothoracic limb bud at stage 7.7. Branching filopodia can be observed, and the length and density of growth cone filopodia are sufficient to occupy the entire lumen for GFP controls. Little to no filopodia can be detected along the axon for Toll7 knockdown pioneer neuron. **E and F.** 40x confocal images focusing on the prothoracic limb bud at stage 8.0. The length and density of growth cone and axonal filopodia are enough to occupy the entire lumen for GFP controls and little to no filopodia can be detected along the neuron for Toll7 knockdown pioneer neurons. The limb buds are outlined in grey.

Discussion

This study aimed to characterize the development of the peripheral nervous system in the cricket embryonic limb buds, which is largely homologous to the peripheral nervous system development in the grasshopper as well as other closely related Orthoptera specices. Then, the limb bud and peripheral nervous system development was examined under Toll7 knockdown. Toll7 knockdown led to a limb bud volume shrinkage from stage 7.7 to stage 8.0. Furthermore, a decrease in mean Ti1 PN length and volume was detected in the early embryonic development stages (stage 7.5 and stage 7.7) for Toll7 knockdown embryos.

Characterization of Limb Bud Peripheral Nervous System Development

The limb bud peripheral nervous system development in cricket embryos seemed to be largely homologous with that observed in grasshopper embryos. In both grasshopper and cricket embryos, a pair of spherical neuronal cell bodies, named "Ti1 neurons" given its later location in the tibia, would emerge under the epithelial layer at the distal tips of limb buds at around 20% of embryonic development (Bentley and Keshishian, 1982). Ti1 neurons would then form into spindle shapes and extend their axons along the epithelial layer medially. The pathways undertaken by Ti1 pioneer neurons in cricket and grasshopper embryos are similar: the Ti1 axons would travel along the dorsoanterior epithelium for several cell diameters and then make a first turn ventroposteriorly. As the growth cones approach the limb bud base, the Ti1 axons made a second sharp medial turn toward the CNS. The completion of the Ti1 route occurs at around 35% developmental stage for both grasshopper and cricket embryos, and the entire Ti1 pathfinding process happens in a relatively short time window of 8-10 hours (Bentley and Keshishian, 1982).

Interestingly, whereas the grasshopper limb buds have three distinctive guidepost cells (F1, F2 and CT1), only two guidepost cells can be observed in cricket embryos (F1 and CT1). In grasshopper embryos, Ti1 axons travel past F1 cells along the epithelium and do not make their stereotypical first turn until reaching the guidepost cell F2 (Bentley and Keshishian, 1982). In contrast, in cricket embryos in the absence of an F2 guidepost cell, Ti1 axons perform their first turn at the first guidepost cell F1. CT1 guidepost cell pairs, on the other hand, had similar roles and developmental patterns in both grasshopper and cricket embryos. At around 30% development, a pair of symmetrically divided cells (CT1) could be observed near the base of the limb buds and antenna, extending axons toward the CNS lateral motor neurons (LMNs) which are also sending projections into the appendages. LMN and CT1 axonal projections will eventually connect and fasciculate as Ti1 growth cones approach CT1 cell

bodies. As Ti1 growth cones reach CT1, the Ti1 axons then followed the paths established by CT1-LMN projections and eventually connect with CNS units (Berlot and Goodman, 1984).

As Ti1 axons complete their connection with the CNS, femoral chordotonal organs (FCOs) and sensory organ complex (SOKs) sensory neurons start to emerge, with FCO axons targeting the cell F1 and SOK axons targeting the Ti1 cell body pair. The same phenomenon is also observed in grasshopper embryos (Bentley and Keshishian, 1982), suggesting Ti1 and F1 cell bodies' unique guidance qualities in aiding sensory neuron gathering and sensory organ formation is well-conserved. In both grasshopper and cricket embryos, the second pair of pioneer neurons (Ti2) send axonal projection toward CT1 cells, which, at this point, have already performed axonogenesis and fasciculated with lateral motor neuron axons from the CNS. After making contacts with 2 guidepost cells (F3 and F4), Ti2 growth cone would eventually contact CT1 cell bodies, forming the first visible peripheral nerve branch in the limb buds. The above information indicates that the cell bodies of pioneer neurons as well as guidepost cells not only serve as "landmark cells" that redirect growth cones, but also possess attractant signaling properties that are targeted by later-emerged neurons.

Berlot and Goodman (1984) proposed an attractive theory on the molecular mechanisms underlying pioneer pathfinding that combines the "guidepost" theory proposed by Bentley and Keshishian (1982), and the "gradient" theory initially raised by Nardi and Kafatos (1976). Berlot and Goodman (1984) proposed an "adhesion hierarchy" within the orthoptera embryonic limb buds in which the adhesion signals are stronger on the neuronal cell bodies than those on the epithelial cells. As a result, when Ti1 cells are first born, as they are the only neurons in the hollow limb bud lumens and thus the only adhesion signals they can follow are that from the epithelial cells. Their axons adhere to the epithelium while the growth cone explores medially. As the first guidepost cell F1 is born, the adhesion signals on this premature sensory neuron are prioritized over those from the epithelial cells and draw the Ti1 growth cone toward its cell bodies. Similarly, the emergence of the second guidepost cell CT2 attracts the growth cones further due to its adhesion signals. It is worth noting that the adhesion signals on the CNS cells are the strongest (Berlot and Goodman, 1984); therefore, all peripheral growth cones will be eventually led to fasciculate with the CNS axons. It is likely that the later emerged sensory neurons (the second pair of pioneer neurons Ti2, their guidepost cells F3 and F4, tarsal neurons, FCO/SGO sensory neurons, etc.) follow the same adhesion hierarchy paradigm. The FCO sensory neurons, for example, emerge 2-3 cell body diameters away from the guidepost cell F1. Since the F1 cell is the closest neuron and presents the strongest adhesion signals, the FCO neurons project axons toward

F1 cell body. Similarly, subgenual organ (SGO) neurons are born about 20 um distally away from the Ti1 cell body pair. Due to the proximity of the SGO neurons to the Ti1 cell bodies and the stronger presence of adhesion signals, the SGO growth cones are directed toward Ti1 cell bodies, and the sensory organ complex (SOK, including subgenual organ and either tympanal organ or tracheal organ) would subsequently gather there. Both FCOs and SGOs are mechanical sensors that process the sensory information of stretch and vibrations (Bentley and Keshishian, 1982). Compellingly, the F1 guidepost cell would eventually become a multipolar sensory neuron that is morphologically and functionally similar to invertebrate multipolar stretch receptors (Bentley and Keshishian, 1982). This suggests guidepost cells' immense morphological and functional versatility, illustrating the high efficiency in the developing nervous system.

Why do cricket embryos have one less guidepost cells than grasshopper embryos? Since in grasshopper embryos, Ti1 axons do not perform their first turn until reaching the guidepost cell F2 and FCO sensory neurons specifically target the F1 guidepost cell, it could be hypothesized that the F1 and F2 cells have distinctive roles in terms of limb bud peripheral nervous system development. Whereas the F1 guidepost cell primarily aids the FCO sensory neuronal targeting, F2 guidepost cells' primary role is to redirect the Ti1 growth cone toward the CNS. In cricket embryos, the F1 cell may be responsible for both the above functions. This is probably due to the morphological differences in the grasshopper and cricket limb buds. Grasshopper embryonic limb buds are much larger than cricket embryonic limb buds at every developmental stage. The grasshopper metathoracic limb bud is able to reach a length of 200 um by 25% of development (Bentley et. al, 1979). The cricket embryonic metathoracic limb bud, in contrast, only reaches a maximum length of 140 um by 25% of development. The pioneer pathway is essential because at early stages of embryonic development, the distance between the Ti1 cell bodies and the CNS is relatively small (<200 um in grasshopper embryos and <150 um in cricket embryos). And the proximity is what makes the growth cone detection of the CNS attractant signals possible. In order to ensure the correct partnering of later emerging sensory neurons in the CNS neurons, a guiding pathway must be established before drastic elongation of appendages caused by rapid epithelial cell division (Bentley and Keshishian, 1982). Since grasshopper embryonic limb buds are longer in shape, an extra guidepost cell might be necessary for the longer pioneer growth cone exploration pathway. Since cricket embryonic limb buds are smaller in sizes, extra attractant signaling on a separate guidepost cell, therefore, is likely not needed.

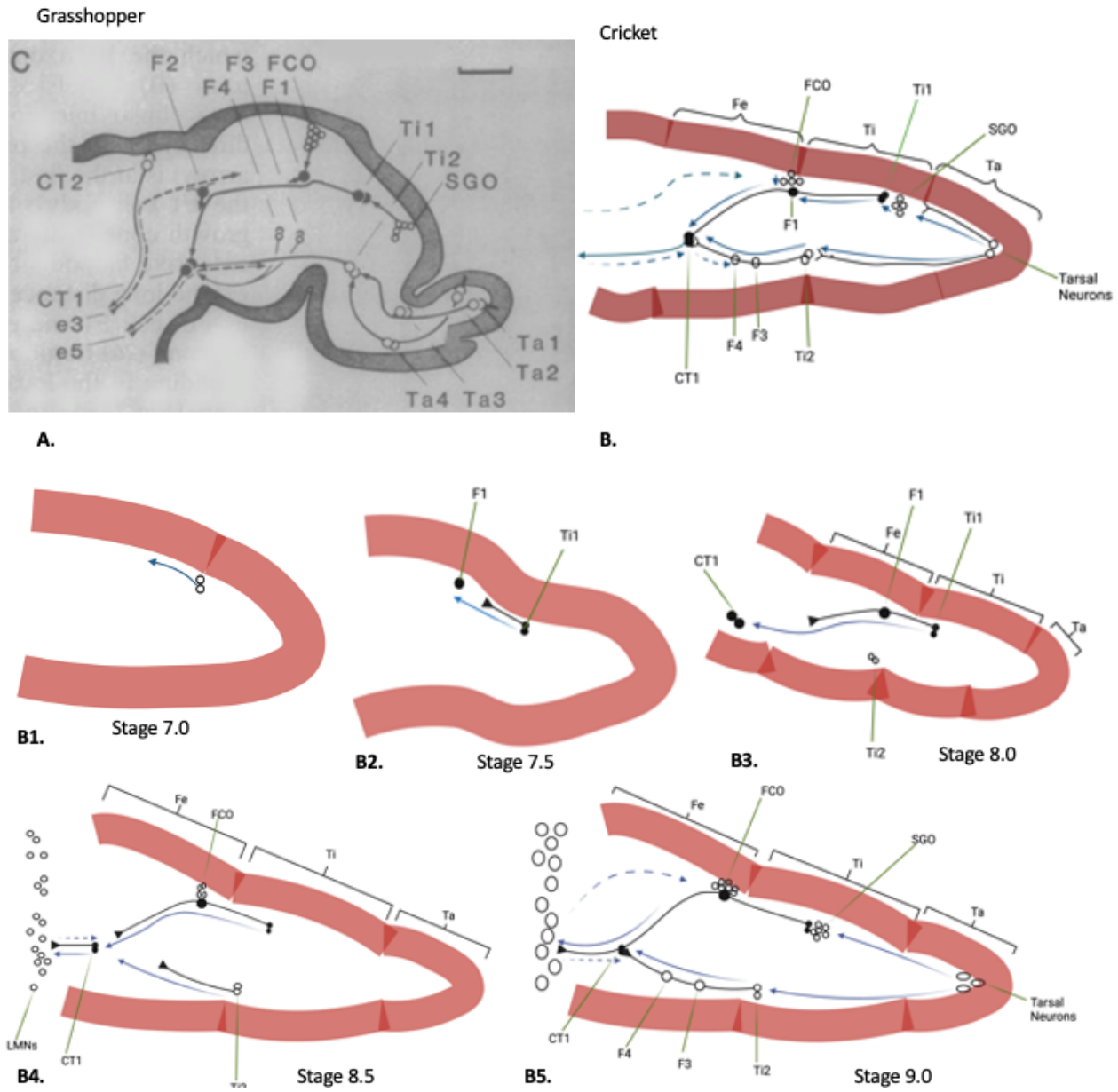

Figure 14. Comparison of the Nerve Pathways at around 45% Embryonic Development. **A.** Peripheral nerve pathway in grasshopper limb buds. Adapted from Bentley and Keshishian (1982). **B.** A schematic drawing of the peripheral nerve pathway in the cricket limb bud. Created by Biorender.com. Solid lines indicate afferent axons and dashed lines indicates efferent axons. Filled cells are the first pair of pioneer neurons and their guidepost cells along the pathway. Fe: femoral segment. Ti: tibial segment. Ta: tarsal segment. FCO: femoral chordotonal organ. SOK: sensory organ complex. SGO: subgenual organ. B1 to B5 illustrates the peripheral nervous system development in the cricket embryonic limb buds from stage 7.0 to stage 9.0.

Figure 14 provides a schematic comparison of limb bud nervous system development in the grasshopper and cricket embryos. Note that cricket embryonic limb buds have much shorter tarsus.

Furthermore, whereas grasshopper Ti1 pioneer axons take a sharp, almost 90° inward turn upon reaching the second guidepost cell F2, the cricket Ti1 pioneer axons' first turn is much milder with a 45° to 60° angle. Besides the lack of F2 guidepost cell and some slight morphological differences in limb bud segmentation and pioneer neuronal pathway, the developmental patterns in the cricket embryonic limb buds are largely homologous to that observed in grasshopper embryos (**Fig.14).**

Toll7 Knockdown Leads to Limb Bud Shrinkage

The results show that Toll7 knockdown results in limb buds volume of smaller volumes, which is evident starting from stage 7.7. The Toll7 mRNA was found to expressed in limb buds in bands in cricket embryos (Al Musawi and Horch, 2022), and a similar Toll expression patterns in limb buds were also found in *Tribolium castaneum* beetles and *Parasteatoda tepidariorum* spiders (Benton et. al, 2016). Stripe-like expression patterns of Toll genes are likely related to cell-cell intercalation, which is defined as the rearrangement of existent epithelial cells that leads to narrowing in one dimension and lengthening in another dimension (usually the perpendicular dimension) (Keller et. al, 2000). Toll7 and Toll10 double knockdown beetle embryos were found to have shortened germbands and appendages but normal limb bud segmentation. Similarly, Toll7 knockdown spider embryos also exhibited shortened and deformed limb buds and severely widened and shortened germbands, indicating conserved axis elongation roles of some Toll receptors in a wide range of arthropods species (Benton et. al, 2016). Therefore, reduction of Toll7 expression might have disrupted cell intercalation, contributing to the smaller limb bud volumes observed in Toll7 knockdown cricket embryos. Since limb bud volume shrinkage was not observed in stage 7.0 to stage 7.5 Toll7 knockdown embryos, it could be deduced that only limb bud elongation was impacted, but not limb bud initiation. In other words, Toll signaling pathway aids the maintenance of cell-cell intercalation process, rather than the initiation of it.

In addition to Toll7, other Toll receptors likely influence appendage development. In beetles, Toll6, Toll8, and Toll10 all exhibit similar band-like expressional patterns in the appendages (limb buds and antennas), suggesting they also play a role in regulating embryonic appendage development and axis elongation. Indeed, bioinformatic analysis indicates that the above Toll receptor proteins are unique for their clade in which they all have significantly longer leucine-rich regions (LRRs) than other Tolls. Therefore, Benton et. al (2016) named this specific group of Tolls "the long toll clade" (or "Loto"). In the current experiment, despite a statistically significant decrease in limb bud volumes induced by Toll7 dsRNA, no additional morphological

differences were observable with brightfield and confocal microscopy. Since it is likely that Toll receptors within the "long toll clade" present similar functionalities, and that several "long tolls" (Toll6-1, Toll6-2, Toll7 and Tollo) are found in crickets, knockdown of two or more genes within the group might result in a more pronounced morphological outcome. In beetle embryonic models, previous experiments showed that the knockdown of either Toll7 or Toll10 did not substantially affect hatching rate or morphological appearances of embryos. However, a simultaneous knockdown of both genes resulted in a drastic decline in hatching rate and visible defects in embryonic morphology. Live imaging portrayed that the morphological defects were likely due to the disruption in cell-cell intercalation (Benton et. al, 2016). Hence, in future experiments, it is of interest to perform double knockdown of Tolls within the "long toll clade."

Toll7 Knockdown Leads to Delayed Pioneer Neuron Development and Decreased Filopodia Density in the Early Developmental Stages

Our results showed that after Toll7 knockdown, the length of pioneer neurons was significant reduced only at stage 7.5 and the volume of pioneer neurons was significantly reduced at stages 7.5 and 7.7. At stage 8.0, however, no significant differences in either the length or the volume of the pioneer neurons were detected.

At stage 7.5 in GFP control embryos, most Ti1 pioneer neuronal pairs have polarized, meaning that the cell bodies have become spindle shaped and axons have started to extend along the epithelial wall. For Toll7 knockdown embryos at this stage, on the other hand, most Ti1 cell bodies still displayed a spherical shape and axonogenesis has not been initiated. Thus, a delay in pioneer neuron axonogenesis might be able to explain the reduction in length and volume under Toll7 knockdown.

It is interesting to note that at stage 7.7, no statistically significant differences were detected by a two-way ANOVA on pioneer axonal lengths between GFP controls and Toll7 knockdown embryos, but a pronounced statistical significance ($p<0.0001$) was detected on the pioneer neuronal volumes between the two groups. This suggests that the larger volumes observed in GFP controls are most likely due to a larger density of filopodia. Indeed, as shown in figure 12, at stage 7.5 and stage 7.7, a much higher percentage of embryonic limb buds in the GFP control groups had voluminous, branching filopodia that covered the entire limb bud lumen as compared to Toll7 knockdown embryos.

Neurotrophic factors in mammals have been shown to promote neuronal precursor cell proliferation (ElShamy and Ernfors, 1997) and axonogensis (Barnett et. al, 2002). Knockdown or knockout of one or multiple neurotrophic factors would result in reduced number and delayed birth time of neuronal precursor cells as well as axonogenesis delay or failure, which is similar to what was observed for Ti1 pioneer neurons with Toll7 knockdown in cricket embryos. In Drosophila models, it was widely observed that Toll6 and Toll7 mutant embryos exhibit significantly decreased neurogenesis and motor axonal targeting in the central nervous system (Mclloy et. al, 2013). Evidence also showed that the Toll6 and Toll7 ligands Spaetzles2 and 5 (DNT1 and DNT2) are able to interact and bind to kek-6, a TrK-family receptor, to activate tyrosine kinase (TyrK) signaling pathway to promote axonogenesis and synaptogenesis, especially at the neuromuscular junctions (NMJs) of the *Drosophila* peripheral nervous system (Ulian-Benitez et. al, 2017). The above evidence suggests that the Toll-Spaetzle actions in crickets is consistent with neurotrophic signaling qualities. Therefore, in the current experiment, a Toll7 knockdown might have deprived of the neurotrophic-like factor Spaetzle's binding partner, causing disrupted and delayed neurogenesis and axonogenesis in the peripheral pioneer neurons as observed in stage 7.5 embryos. It would be of interest for the future experiments to knockdown Toll7's binding ligand Spaetzle 2 and 5 too to see if similar results could be yielded.

It is notable that with Toll7 knockdown, axonal extension rates seemed to be affected. Axonal elongation is achieved by microtubule rearrangement. A growth cone explorative pause occurs when microtubule fragments perform a loop-like movement within the growth cone. In response to developmental cues, the sporadic microtubule fragments would gather and mobilize toward the desired locations, thus extending the axons (Dent et. al, 2003). Recent discoveries revealed that Toll receptors in *Drosophila* plays an important role in regulating microtubule dynamics. Toll6 was found to promote the expression of nuclear FoxO by inhibiting Akt pathways. FoxO is a protein that was previously found to play a cardinal role in regulating microtubule organization and stability. *Drosophila* lacking FoxO displayed disorganized microtubule fragments and strengthened microtubule stability at motor axonal growth cones (Nechipurenko and Broihier, 2012). Unsurprisingly, the knockdown of Toll6 in Drosophila models illustrated a similar phenomenon at neuromuscular junctions (NMJs), further confirming the interactive relationship between Toll receptors and FoxO proteins (McLaughlin et. al, 2016). In the current experiment, the shortened pioneer axon phenotype seen with Toll7 knockdown is

consistent with an enhanced microtubule stability at the growth cone. The strengthened microtubule stability would strongly reduce microtubule fragment mobility, therefore impeding axonal extension and elongation.

A notable decrease in filopodia density was also observed under Toll7 knockdown from stage 7.5 to stage 8.0. Filopodia are the fine long filaments that extends primarily from the growth cones, but also from the cell bodies and along the axons. Filopodia were determined *in vivo* to be responsible for grasshopper limb bud pioneer neuron growth cone steering, but not pioneer axon elongation (Bentley and Toroian-Raymond, 1986). Filopodia exploration is mainly made possible by filopodia filaments' microscopic sizes. Each filopodia filament contains voltage-gated calcium channels. Given the extremely small cytoplasmic capacity, the Ca2+ thresholds on filopodia filaments are extraordinarily low, meaning that even a small change in intracellular concentration would lead to elicitation of a relevant biological signal (Kater and Rehder, 1995). The above unique qualities make filopodia highly sensitive to environmental signals, including developmental cues and neurotrophic factors. Mammalian neurotrophic factors, such as nerve growth factors (NGFs), are widely recognized for their preeminent role in inducting axonal filopodia growth. It is suggested from the current experiment that the Toll-Spaetzle pathway seems to exhibit NGF-like properties, since Toll7 knockdown prominently reduced filopodia density on the Ti1 pioneer neurons in cricket embryonic limb buds. Nerve growth factors promote filopodia growth by altering axonal cytoskeletal events. A fraction of simultaneously emerging transient filamentous actin (F-actin) patches give rise to the filopodia filaments. NGF was found to increase the emergence rate of F-actin patches but not the fraction of patches that give rise to filopodia filaments (Ketschek and Gallo, 2010). The Toll-Spaetzle pathway might also influence filopodia density via similar mechanisms of modifying cytoskeleton activity. As mentioned before, Drosophila Tolls could potentially enhance microtubule activity, and microtubules were found to be important in pioneer neuron filopodia exploration. Microtubules were found to accrue at areas with high concentrations of F-actin due to a possible microtubule-F-actin linkage (Bentley and O' Connor, 1994). An enhanced stability in microtubule activities induced by Toll7 knockdown, therefore, would likely result in failure in microtubule accrual at F-actin-rich sites, subsequently leading to failure in filopodia stabilization. In summary, the current experiment provides another appealing evidence of neurotrophic properties provided by the Toll-Spaetzle pathway.

It is intriguing to observe that the Toll7 knockdown effects seemed to diminish around stage 8.0, and that no additional observable developmental differences were observed in PNS development in later stages. Several theories might be able to explain this phenomenon. First, dsRNA silencing of the Toll pathway might function in an age-dependent manner, and it is possible that the dsRNA materials would degrade after a period of time. Toll pathway silencing by direct dsRNA injection was found to be only efficient in 4 days or older fruit flies, and the knockdown effect may not last more than a week (Goto et. al, 2003). Therefore, it is likely that the expressional depression exerted by Toll7 dsRNA was no longer effective by cricket embryonic development stage 8.0, which is about a week from initial dsRNA injection. Second, compensatory molecular pathways might have been elicited after a while of Toll7 expressional depression. Previous qPCR studies in our lab have found an increase in Toll6 and Toll7 expression from stage 6.0 to stage 8.0 embryos under normal development. Therefore, it is possible that the later upregulation of Toll7 overwhelms the dsRNA, leading to a recovery of peripheral nervous system development in later stages. Second, additional molecular pathways might have eventually compensated for the reduction in Toll7 expressional level. For example, perhaps that Toll6 compensated the deficiency in Toll7 and redirected the embryonic peripheral nervous system into normal development. Toll6 and Toll7 are structurally and functionally similar. They both exhibited longer leucine-rich regions (LRRs) than other Tolls (Benton et. al, 2016). Furthermore, neurotrophin-like factor Spaetzle is able to promiscuously bind to both Toll6 and Toll7 receptors in Drosophila (Mclloy, et. al, 2013). Previous experiments also demonstrated that manipulation of Toll6 or Toll7 alone can cause dendrites-axons mismatching in drosophila olfactory circuits, suggesting that Toll6 and Toll7 are both powerful axonal targeting factor that is capable of outcompeting other partnering factors (Ward et. al, 2015).

Future Directions

Since we are not certain about dsRNA's half-life and whether the upregulation in Toll7's expressional level in normal developing embryos impacts dsRNA knockdown in embryos, a qPCR study on the Toll7 knockdown embryos might be necessary. If qPCR results indicate that Toll7 expression is upregulated across development stages despite RNA interference, the injection of a higher inititial concentration or a booster injection at later stages could be considered. On the other hand, if qPCR results indicate persistently low Toll7 expressional level

throughout developmental stages, it is more likely that a compensatory pathway is involved. Under this circumstance, a simultaneous knockdown of two or more Toll genes might be favored, especially given previous findings that morphological defects in arthropods were not detected until a double knockdown of two Toll genes was performed (Benton et. al, 2016). Compellingly, in a beetle model, the knockdown of Toll7 in the embryos leads to postembryonic behavioral defects (Benton et. al, 2016). Hence, it might also be interesting to hatch some Toll7 knockdown cricket embryos and observe any deviant postembryonic behaviors.

Furthermore, although filopodia density is visibly higher in GFP controls than in Toll7 knockdown embryos, it might be beneficial to quantify filopodia filament number. This can be achieved with software programs such as Imaris 10 Filament Tracer, which allows 3D reconstruction of neuron arborization analysis.

Finally, in the current experiment, we observed a shrinkage in limb bud volumes under Toll7 knockdown which is possibly related to cell-cell intercalation. We also observed a delay in pioneer neuron development in early embryonic stages that is potentially linked to cytoskeletal regulation. However, we are not sure if these two observations are connected. Therefore, it is of interest for future studies to explore and compare the mechanisms of the Toll signaling pathway regulating epithelial and neuronal cell development to determine if the same molecular pathway is involved in the developmental modulation of both cell types.

References

Auld, V. (1999). Glia as mediators of growth cone guidance: studies from insect nervous systems. *Cellular and Molecular Life Sciences CMLS*, *55*(11), 1377-1385.

Bainbridge, S. P., & Bownes, M. (1981). Staging the metamorphosis of Drosophila melanogaster.

Barnett, M. W., Fisher, C. E., Perona-Wright, G., & Davies, J. A. (2002). Signalling by glial cell line-derived neurotrophic factor (GDNF) requires heparan sulphate glycosaminoglycan. *Journal of Cell Science*, *115*(23), 4495-4503.

Bate, C. M. (1976). Pioneer neurones in an insect embryo. *Nature*, *260*(5546), 54-56.

Bentley, D., & Keshishian, H. (1982). Pathfinding by peripheral pioneer neurons in grasshoppers. *Science*, *218*(4577), 1082-1088.

Bentley, D., Keshishian, H., Shankland, M., & Toroian-Raymond, A. (1979). Quantitative staging of embryonic development of the grasshopper, Schistocerca nitens.

Bentley, D., & O'Connor, T. P. (1994). Cytoskeletal events in growth cone steering. *Current opinion in neurobiology*, *4*(1), 43-48.

Bentley, D., & Toroian-Raymond, A. (1986). Disoriented pathfinding by pioneer neurone growth cones deprived of filopodia by cytochalasin treatment. *Nature*, *323*(6090), 712-715.

Benton, M. A., Pechmann, M., Frey, N., Stappert, D., Conrads, K. H., Chen, Y. T., ... & Roth, S. (2016). Toll genes have an ancestral role in axis elongation. *Current Biology*, *26*(12), 1609-1615.

Berlot, J., & Goodman, C. S. (1984). Guidance of peripheral pioneer neurons in the grasshopper: adhesive hierarchy of epithelial and neuronal surfaces. *Science*, *223*(4635), 493-496.

Bier, E. (1997). Anti-neural-inhibition: a conserved mechanism for neural induction. *Cell*, *89*(5), 681-684.

Cabrera, C. V., Martinez-Arias, A., & Bate, M. (1987). The expression of three members of the achaete-scute gene complex correlates with neuroblast segregation in Drosophila. *Cell*, *50*(3), 425-433.

Campos-Ortega, J. A. (1995). Genetic mechanisms of early neurogenesis inDrosophila melanogaster. *Molecular neurobiology*, *10*(2), 75-89.

Deng, W. M., & Bownes, M. (1997). Two signalling pathways specify localised expression of

the Broad-Complex in Drosophila eggshell patterning and morphogenesis. *Development*, *124*(22), 4639-4647.

Dent, E. W., Tang, F., & Kalil, K. (2003). Axon guidance by growth cones and branches: common cytoskeletal and signaling mechanisms. *The Neuroscientist*, *9*(5), 343-353.

Donoughe, S., & Extavour, C. G. (2016). Embryonic development of the cricket Gryllus bimaculatus. *Developmental Biology*, *411*(1), 140-156.

Edwards, J. S., Chen, S. W., & Berns, M. W. (1981). Cercal sensory development following laser microlesions of embryonic apical cells in Acheta domesticus. *Journal of Neuroscience*, *1*(3), 250-258.

Edwards, J. S., & Chen, S. W. (1979). Embryonic development of an insect sensory system, the abdominal cerci ofAcheta domesticus. *Wilhelm Roux's archives of developmental biology*, *186*(2), 151-178.

ElShamy, W. M., & Ernfors, P. (1997). Brain-derived neurotrophic factor, neurotrophin-3, and neurotrophin-4 complement and cooperate with each other sequentially during visceral neuron development. *Journal of Neuroscience*, *17*(22), 8667-8675.

Goodman, C. S., & Bate, M. (1981). Neuronal development in the grasshopper. *Trends in neurosciences*, *4*, 163-169.

Goto, A., Blandin, S., Royet, J., Reichhart, J. M., & Levashina, E. A. (2003). Silencing of Toll pathway components by direct injection of double-stranded RNA into Drosophila adult flies. *Nucleic acids research*, *31*(22), 6619-6623.

Foldi, I., Anthoney, N., Harrison, N., Gangloff, M., Verstak, B., Nallasivan, M. P., ... & Hidalgo, A. (2017). Three-tier regulation of cell number plasticity by neurotrophins and Tolls in Drosophila. *Journal of Cell Biology*, *216*(5), 1421-1438.

Howard, L. J., Brown, H. E., Wadsworth, B. C., & Evans, T. A. (2019, January). Midline axon guidance in the Drosophila embryonic central nervous system. In *Seminars in cell & developmental biology* (Vol. 85, pp. 13-25). Academic Press.

Imler, J. L., & Hoffmann, J. A. (2001). Toll receptors in innate immunity. *Trends in cell biology*, *11*(7), 304-311.

Jacobs, J. R. (2000). The midline glia of Drosophila: a molecular genetic model for the developmental functions of glia. *Progress in neurobiology*, *62*(5), 475-508.

Keller, R., Davidson, L., Edlund, A., Elul, T., Ezin, M., Shook, D., & Skoglund, P. (2000).

Mechanisms of convergence and extension by cell intercalation. *Philosophical Transactions of the Royal Society of London. Series B: Biological Sciences*, *355*(1399), 897-922.

Keshishian, H. (1980). The origin and morphogenesis of pioneer neurons in the grasshopper metathoracic leg. *Developmental biology*, *80*(2), 388-397.

Keshishian, H., & Bentley, D. (1983). Embryogenesis of peripheral nerve pathways in grasshopper legs: I. The initial nerve pathway to the CNS. *Developmental biology*, *96*(1), 89-102.

Ketschek, A., & Gallo, G. (2010). Nerve growth factor induces axonal filopodia through localized microdomains of phosphoinositide 3-kinase activity that drive the formation of cytoskeletal precursors to filopodia. *Journal of Neuroscience*, *30*(36), 12185-12197.

Lewis, M., Arnot, C. J., Beeston, H., McCoy, A., Ashcroft, A. E., Gay, N. J., & Gangloff, M. (2013). Cytokine Spätzle binds to the Drosophila immunoreceptor Toll with a neurotrophin-like specificity and couples receptor activation. *Proceedings of the National Academy of Sciences*, *110*(51), 20461-20466.

McIlroy, G., Foldi, I., Aurikko, J., Wentzell, J. S., Lim, M. A., Fenton, J. C., ... & Hidalgo, A. (2013). Toll-6 and Toll-7 function as neurotrophin receptors in the Drosophila melanogaster CNS. *Nature neuroscience*, *16*(9), 1248-1256.

McLaughlin, C. N., Nechipurenko, I. V., Liu, N., & Broihier, H. T. (2016). A Toll receptor–FoxO pathway represses Pavarotti/MKLP1 to promote microtubule dynamics in motoneurons. *Journal of Cell Biology*, *214*(4), 459-474.

Meier, T., & Reichert, H. (1995). Developmental mechanisms, homology and evolution of the insect peripheral nervous system. *The Nervous Systems of Invertebrates: An Evolutionary and Comparative Approach: With a Coda written by TH Bullock*, 249-271.

Miyamoto, T., & Shimozawa, T. (1983). Embryonic Development of the Central Nervous System in the Cricket, Gryllus bimaculatus I. Segmental Homologies in Early Neurogenesis. *動物学雑誌*, *92*(3), 317-331.

Nakamoto, M., Moy, R. H., Xu, J., Bambina, S., Yasunaga, A., Shelly, S. S., ... & Cherry, S. (2012). Virus recognition by Toll-7 activates antiviral autophagy in Drosophila. *Immunity*, *36*(4), 658-667.

Nardi, J. B., & Kafatos, F. C. (1976). Polarity and gradients in lepidopteran wing epidermis: I.

Changes in graft polarity, form, and cell density accompanying transpositions and reorientations.

Nechipurenko, I. V., & Broihier, H. T. (2012). FoxO limits microtubule stability and is itself negatively regulated by microtubule disruption. *Journal of Cell Biology*, *196*(3), 345-362.

Parthier, C., Stelter, M., Ursel, C., Fandrich, U., Lilie, H., Breithaupt, C., & Stubbs, M. T. (2014). Structure of the Toll-Spätzle complex, a molecular hub in Drosophila development and innate immunity. *Proceedings of the National Academy of Sciences*, *111*(17), 6281-6286.

Parker, J. S., Mizuguchi, K., & Gay, N. J. (2001). A family of proteins related to Spätzle, the toll receptor ligand, are encoded in the Drosophila genome. *Proteins: Structure, Function, and Bioinformatics*, *45*(1), 71-80.

Rickert, C., Kunz, T., Harris, K. L., Whitington, P. M., & Technau, G. M. (2011). Morphological characterization of the entire interneuron population reveals principles of neuromere organization in the ventral nerve cord of Drosophila. *Journal of Neuroscience*, *31*(44), 15870-15883.

Shankland, M. (1981). Development of a sensory afferent projection in the grasshopper embryo: I. Growth of peripheral pioneer axons within the central nervous system.

Singhania, A., & Grueber, W. B. (2014). Development of the embryonic and larval peripheral nervous system of Drosophila. *Wiley Interdisciplinary Reviews: Developmental Biology*, *3*(3), 193-210.

Slifer, E. H., & Sekhon, S. S. (1975). The femoral chordotonal organs of a grasshopper, Orthoptera, Acrididae. *Journal of Neurocytology*, *4*(4), 419-438.

Sun, B., & Salvaterra, P. M. (1995). Characterization of nervana, a Drosophila melanogaster neuron-specific glycoprotein antigen recognized by anti-horseradish peroxidase antibodies. *Journal of neurochemistry*, *65*(1), 434-443.

Skeath, J. B., Panganiban, G., Selegue, J., & Carroll, S. B. (1992). Gene regulation in two dimensions: the proneural achaete and scute genes are controlled by combinations of axis-patterning genes through a common intergenic control region. *Genes & Development*, *6*(12b), 2606-2619.

Sonnenfeld, M. J., & Jacobs, J. R. (1995). Apoptosis of the midline glia during Drosophila embryogenesis: a correlation with axon contact. *Development*, *121*(2), 569-578.

Ulian-Benitez, S., Bishop, S., Foldi, I., Wentzell, J., Okenwa, C., Forero, M. G., ... & Hidalgo, A. (2017). Kek-6: a truncated-Trk-like receptor for Drosophila neurotrophin 2 regulates structural synaptic plasticity. *PLoS genetics*, *13*(8), e1006968.

Ward, A., Hong, W., Favaloro, V., & Luo, L. (2015). Toll receptors instruct axon and dendrite targeting and participate in synaptic partner matching in a Drosophila olfactory circuit. *Neuron*, *85*(5), 1013-1028.

Weigel, M., Wang, L., & Fu, M. M. (2021). Microtubule organization and dynamics in oligodendrocytes, astrocytes, and microglia. *Developmental Neurobiology*, *81*(3), 310-320.

Wolf, N., Regan, C. L., & Fuller, M. T. (1988). Temporal and spatial pattern of differences in microtubule behaviour during Drosophila embryogenesis revealed by distribution of a tubulin isoform. *Development*, *102*(2), 311-324.